

TOPICAL REVIEW • OPEN ACCESS

# The issues on the commercialization of perovskite solar cells

To cite this article: Lixiu Zhang *et al* 2024 *Mater. Futures* **3** 022101

View the [article online](#) for updates and enhancements.

## You may also like

- [Critical state-induced emergence of superior magnetic performances in an iron-based amorphous soft magnetic composite](#)  
Liliang Shao, Rongsheng Bai, Yanxue Wu et al.
- [Observation of stabilized negative capacitance effect in hafnium-based ferroic films](#)  
Leilei Qiao, Ruiting Zhao, Cheng Song et al.
- [High-brightness green InP-based QLEDs enabled by \*in-situ\* passivating core surface with zinc myristate](#)  
Yuanbin Cheng, Qian Li, Mengyuan Chen et al.

## Topical Review

# The issues on the commercialization of perovskite solar cells

Lixiu Zhang<sup>1</sup>, Yousheng Wang<sup>2</sup>, Xiangchuan Meng<sup>3</sup>, Jia Zhang<sup>8</sup>, Pengfei Wu<sup>5</sup>, Min Wang<sup>6</sup>, Fengren Cao<sup>6</sup>, Chunhao Chen<sup>7</sup>, Zhaokui Wang<sup>7</sup>, Fu Yang<sup>9</sup>, Xiaodong Li<sup>10</sup>, Yu Zou<sup>11</sup>, Xi Jin<sup>12</sup>, Yan Jiang<sup>13</sup> , Hengyue Li<sup>14</sup>, Yucheng Liu<sup>15</sup>, Tongle Bu<sup>16</sup>, Buyi Yan<sup>17</sup>, Yaowen Li<sup>9</sup>, Junfeng Fang<sup>10</sup>, Lixin Xiao<sup>11</sup>, Junliang Yang<sup>14</sup>, Fuzhi Huang<sup>16</sup>, Shengzhong Liu<sup>15</sup>, Jizhong Yao<sup>17</sup>, Liangsheng Liao<sup>7,\*</sup>, Liang Li<sup>6,\*</sup> , Fei Zhang<sup>5,\*</sup>, Yiqiang Zhan<sup>4,\*</sup>, Yiwang Chen<sup>3,\*</sup>, Yaohua Mai<sup>2,\*</sup> and Liming Ding<sup>1,\*</sup> 

<sup>1</sup> Center for Excellence in Nanoscience (CAS), Key Laboratory of Nanosystem and Hierarchical Fabrication (CAS), National Center for Nanoscience and Technology, Beijing 100190, People's Republic of China

<sup>2</sup> Institute of New Energy Technology, College of Information Science and Technology, Jinan University, Guangzhou 510632, People's Republic of China

<sup>3</sup> Institute of Polymers and Energy Chemistry (IPEC), Nanchang University, Nanchang 330031, People's Republic of China

<sup>4</sup> School of Information Science and Technology, Fudan University, Shanghai 200433, People's Republic of China

<sup>5</sup> School of Chemical Engineering and Technology, Tianjin University, Tianjin 300072, People's Republic of China

<sup>6</sup> School of Physical Science and Technology, Soochow University, Suzhou 215006, People's Republic of China

<sup>7</sup> Institute of Functional Nano & Soft Materials (FUNSOM), Soochow University, Suzhou 215123, People's Republic of China

<sup>8</sup> Institute of optoelectronics, Fudan University, Shanghai 200433, People's Republic of China

<sup>9</sup> College of Chemistry, Chemical Engineering and Materials Science, Soochow University, Suzhou 215123, People's Republic of China

<sup>10</sup> School of Physics and Electronic Science, East China Normal University, Shanghai 200241, People's Republic of China

<sup>11</sup> State Key Laboratory for Artificial Microstructure and Mesoscopic Physics, Department of Physics, Peking University, Beijing 100871, People's Republic of China

<sup>12</sup> College of Biophotonics, South China Normal University, Guangzhou 510631, People's Republic of China

<sup>13</sup> School of Materials Science and Engineering, Beijing Institute of Technology, Beijing 100081, People's Republic of China

<sup>14</sup> School of Physics and Electronics, Central South University, Changsha 410083, People's Republic of China

<sup>15</sup> School of Materials Science and Engineering, Shaanxi Normal University, Xi'an 710119, People's Republic of China

\* Authors to whom any correspondence should be addressed.



Original content from this work may be used under the terms of the [Creative Commons Attribution 4.0 licence](https://creativecommons.org/licenses/by/4.0/). Any further distribution of this work must maintain attribution to the author(s) and the title of the work, journal citation and DOI.

<sup>16</sup> State Key Laboratory of Advanced Technology for Materials Synthesis and Processing, Wuhan University of Technology, Wuhan 430070, People's Republic of China

<sup>17</sup> Microquanta semiconductor, Hangzhou 311121, People's Republic of China

E-mail: [lslliao@suda.edu.cn](mailto:lslliao@suda.edu.cn), [lli@suda.edu.cn](mailto:lli@suda.edu.cn), [fei\\_zhang@tju.edu.cn](mailto:fei_zhang@tju.edu.cn), [yqzhan@fudan.edu.cn](mailto:yqzhan@fudan.edu.cn), [ywchen@ncu.edu.cn](mailto:ywchen@ncu.edu.cn), [yaohuamai@jnu.edu.cn](mailto:yaohuamai@jnu.edu.cn) and [ding@nanocr.cn](mailto:ding@nanocr.cn)

Received 20 December 2023, revised 25 March 2024

Accepted for publication 26 March 2024

Published 18 April 2024



## Abstract

Perovskite solar cells have aroused a worldwide research upsurge in recent years due to their soaring photovoltaic performance, ease of solution processing, and low cost. The power conversion efficiency record is constantly being broken and has recently reached 26.1% in the lab, which is comparable to the established photovoltaic technologies such as crystalline silicon, copper indium gallium selenide and cadmium telluride (CdTe) solar cells. Currently, perovskite solar cells are standing at the entrance of industrialization, where huge opportunities and risks coexist. However, towards commercialization, challenges of up-scaling, stability and lead toxicity still remain, the proper handling of which could potentially lead to the widespread adoption of perovskite solar cells as a low-cost and efficient source of renewable energy. This review gives a holistic analysis of the path towards commercialization for perovskite solar cells. A comprehensive overview of the current state-of-the-art level for perovskite solar cells and modules will be introduced first, with respect to the module efficiency, stability and current status of industrialization. We will then discuss the challenges that get in the way of commercialization and the corresponding strategies to address them, involving the upscaling, the stability and the lead toxicity issue. Insights into the future direction of commercialization of perovskite photovoltaics was also provided, including the flexible perovskite cells and modules and perovskite indoor photovoltaics. Finally, the future perspectives towards commercialization are put forward.

**Keywords:** commercializations, perovskite solar cells, state-of-the-art level, challenges and perspectives, indoor photovoltaics

## 1. Introduction

Perovskite materials have exhibited great potential in photovoltaic fields. Benefiting from their favorable photoelectric properties, including strong light absorption, long carrier diffusion length and high charge carrier mobility, the power conversion efficiency (PCE) of perovskite solar cells (PSCs) has gone through dramatic upswing over the past few years. Recently, the certified PCE has climbed to 26.1% [1], which is the third-highest single-junction photovoltaic technology, just behind GaAs and crystalline silicon solar cells. Except for considerable photovoltaic performance, low cost, solution processibility and flexibility endow PSCs with huge commercial potential, not only in the grid-connected system but also in off-grid scenarios like building integrated photovoltaic (BIPV), wearable electronics and indoor photovoltaics.

Now that PSCs have reached unprecedented progress at lab scale, industrialization and stepping into commercialization are definitely the next steps. Before that, challenges of up-scaling, stability and toxicity need to be tackled first. By far, most of the top-performing devices are based on small-area substrates [2–4]. How to preserve high efficiency

and low batch-to-batch variation during upscaling is the major hurdle because the fabrication techniques of PSCs cannot be directly transferred to perovskite solar modules (PSMs). The current PCE record for small-area device is 26.1%. When scaling up to 1 cm<sup>2</sup>, the efficiency record drops slightly to 24.67% [5]. Further expanding the area will cause even severer efficiency loss. The efficiency record for 810 cm<sup>2</sup> device drops to 19.9% [6]. Large-area modules with all functional layers fabricated by scalable methods are quite limited. The second challenge is stability. Apart from the intrinsic instability of perovskite material itself, perovskite solar cells can be easily deteriorated by external environmental factors like moisture, oxygen, heat, light, radiation, etc. Encapsulation is an effective measure to attenuate the detrimental impacts induced by those factors. Several groups have reported PSCs surpassing the standards of IEC 61 215 qualification tests [7, 8], and over 10 000 h stability has been reported for a 10 × 10 cm<sup>2</sup> printable module under AM 1.5 G illumination [9]. However, towards commercialization, there is still a long way to go. Moreover, toxicity issue regarding lead cannot be neglected. Concerns about the damage of lead leakage to human health and water resources will slow down or even impede the commercialization course. Although encapsulation can reduce

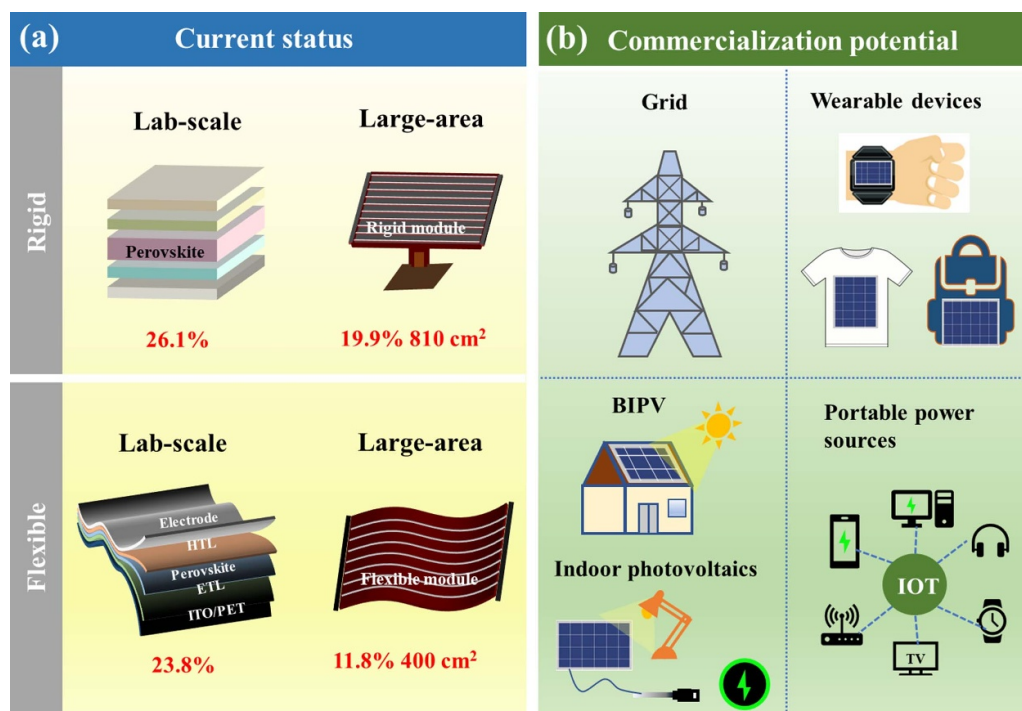


**Figure 1.** The path towards commercialization, in terms of (a) current status and (b) promising applications of commercialization.

the probability of lead leakage to a certain extent, the exploration of Pb-free or Pb-less materials can solve the toxicity problem from the root, which is still worth trying. Besides, module recycling is an effective way to reduce contamination and lead waste, which is desirable for the sustainable development of PSCs.

To enter the already mature photovoltaic market represented by Si solar cells, one plausible approach is to construct tandem solar cells with them to make full of the well-established production lines, which can break through the efficiency limit of single-junction solar cells and increase the overall power output of the module per unit area. Impressively, the PCE for perovskite-Si tandem solar cells have been improved to 33.9% by LONGi company, which further increase the potential of perovskite solar cells towards commercialization [1]. However, towards commercialization, perovskite-Si tandem solar cells are faced with harsher requirements for the stability, scale-up and cost control. The levelized cost of energy (LCOE) should be lower than that of commercial silicon solar cells. Since there has been a great many works analyzing the commercial potential of perovskite tandem solar cells [10–12], here we mainly focus on the commercialization issues of perovskite solar cell itself. Another way is to differentiate the market positioning of perovskite solar cells to distinguish itself from other photovoltaic technologies. Light weight, low temperature production and flexibility allow PSCs to be integrated on flexible substrates, expanding their application to various scenarios, such as building integrated photovoltaics, portable products, wearable electronics, and near-space applications, etc (figure 1). Besides, flexible perovskite solar cells are compatible with cost-effective roll-to-roll mass production, further adding their market competitiveness.

Recently, an impressive champion PCE of 23.8% has been achieved for lab-scale flexible PSCs [13], opening up market breakthrough point. In addition, indoor photovoltaics is another promising direction, which increases the energy utilization efficiency by offering supplemental power source to indoor electronics. It can be integrated into various devices and applications in internet of things (IoT) systems, including wireless sensors, smart home devices, and wearable electronics, providing a reliable and convenient source of power (figure 1).

In this review, an overall analysis of the commercialization path of PSCs is provided. Initially, the current status of commercialization is briefly introduced. Secondly, the three primary remaining challenges that hinders the commercialization process are elaborated respectively, including up-scaling, stability and toxicity. Next, effective encapsulation strategies and encapsulation materials are introduced. Whereafter, promising directions of commercialization that differentiate PSCs with the well-established Si solar cells production line are discussed, including flexible devices and indoor photovoltaics. Finally, a conclusion and outlook for the commercialization of PSCs in the foreseeable future is provided.

## 2. Current status of industrialization

As many countries around the world have put forward the ‘zero carbon’ or ‘carbon neutral’ climate goals, the development of renewable energy represented by photovoltaic has become a global consensus. As the photovoltaic performance of perovskite solar cells continually hit record highs, they have

**Table 1.** Confirmed record efficiency results of perovskite-related photovoltaics, [5, 6, 18] measured under the global AM1.5 spectrum ( $1000 \text{ W m}^{-2}$ ) at  $25^\circ \text{C}$  (IEC 60 904–3: 2008 or ASTM G-173-03 global).

Classification	Efficiency (%)	Area ( $\text{cm}^2$ )	Organization
Perovskite (cell)	$26.1 \pm 0.6$	0.05127 (da)	U. of Science and Technology of China
Perovskite (cell)	24.67	1.0053 (ap)	Shenzhen Infinite Solar Tech.
Perovskite (minimodule)	$22.4 \pm 0.5$	26.02 (da)	EPFLSion/NCEPU, 8 cells
Perovskite (module)	$18.6 \pm 0.7$	809.9 (da)	UtmoLight (39 cells)
Perovskite/Si	$33.7 \pm 1.1$	1.0035 (da)	KAUST, 2-term.
Perovskite/Si (large)	$28.6 \pm 1.4$	258.14 (t)	Oxford PV, 2-term.
Perovskite/CIGS	$24.2 \pm 0.7$	1.045 (da)	HZB, 2-terminal
Perovskite/perovskite	$29.1 \pm 0.5$	0.0489 (da)	Nanjing U, 2-term.
Perovskite/perovskite (minimodule)	$24.5 \pm 0.6$	20.25 (da)	NanjingU/Renshine, 2-term.
Perovskite/organic	$23.4 \pm 0.8$	0.0552 (da)	NUS/SERIS, 2-term.

Abbreviations: (da), designated illumination area; (ap), aperture area; (t), total area.

become the most eye-catching topic in photovoltaic field these years. In the industry community, perovskite solar cell start-ups have emerged like mushrooms after rain and have obtained financing through the primary market, becoming a new favorite of the capital market. The production lines of perovskite solar cell enterprises are advancing rapidly with the advancement of processing techniques and the continuous investment enthusiasm of industrial capital. With the collaborative efforts of academia and industry, both the module efficiency and stability are dramatically enhanced [14–17]. Perovskite solar cells are in the middle of industrialization.

### 2.1. Module efficiency

Companies and organizations are actively contributing to the efficiency improvement of perovskite solar cells and modules, as listed in table 1. For  $1.0053 \text{ cm}^2$  PSCs, which represents a tipping point from small area to large area, the efficiency record has been improved to 24.67% by Shenzhen Infinite Solar Technology CO., LTD [5]. When scaling up to  $26.02 \text{ cm}^2$  module, the efficiency drops to 22.4% [18]. Modules with area larger than  $100 \text{ cm}^2$  and fabricated by up-scalable methods (such as blade coating, slot-die coating, inkjet printing, and spray coating) are quite limited. According to NREL, the highest record for large-scale perovskite solar modules was 19.9% with an active area of  $810 \text{ cm}^2$  by UtmoLight company [6]. Notably, the PCE of Perovskite/Si tandem solar cells has reached 33.2% for small-area devices and 26.8% for large-area devices, which opens up a new way for entering the Si-cell-dominated market.

### 2.2. Module stability

The stability of perovskite modules determines the PV system life time to a great extent and also affects the system LCOE cost. Perovskite module is the latest solar technology and there is currently no specialized IEC standard to test its stability. However, perovskite modules can follow the IEC 61 215, which is designed for silicon or other thin film technologies.

Few companies have made attempts to do the IEC tests. In table 2, we list several reported IEC test results.

**Table 2.** The reported perovskite module stability test results for companies.

Organization	Test classification	Type	Result
Microquanta	IEC 61215/61730	Test sequence	Pass
GCL- Perovskite	Ball drop test	Individual	Pass

**Table 3.** The perovskite production line statuses from perovskite companies.

Organization	Capacity	Type	Status
Microquanta	120 MW	Single-junction	Full capacity production [19]
GCL- Perovskite	100 MW	Single-junction	Ramp-up [20]
Oxford PV	100 MW	Perovskite/silicon tandem	Ramp-up [21]
Wondersolar	200 MW	Carbon-based single-junction	Ramp-up [22]
Utmolight	150 MW	Single-junction	Equipment move-in [23]

### 2.3. Capacity

A large amount of investment is put into the field of perovskite photovoltaics. The production capacity is constantly expanding. Several production line statuses are listed in table 3.

In these perovskite solar cells companies, Micoquanta Semiconductor has released their first commercial perovskite module, called  $\alpha$  perovskite module. The module size is  $1635 \text{ mm} \times 635 \text{ mm} \times 6.5 \text{ mm}$ . The power is up to 130 W.

### 2.4. Real-field perovskite system

It is reported that in July 2022, Microquanta has installed and operated 100 kW perovskite photovoltaic system in Zhejiang Province, China. The system is the first reported grid-connected perovskite solar system on the 100 kW scale (figure 2).





**Figure 2.** Picture of 100 kW perovskite grid-connected solar farm from Micoquanta.

### 2.5. Market prospect

According to the report released by The International Energy Agency, the solar capacity expansion in 2023 was 286 GW, which represents the main source of global renewable capacity expansion [24]. The capacity is anticipated to further increase in 2024, driven by increasing environmental concerns, government incentives, and the declining cost of solar technology. In light of increased electricity prices stemming from the global energy crisis, many countries, particularly in Europe, put forward favorable policies on developing renewable energy to reinforce energy security, which produces a conducive environment for solar PV.

Perovskite solar cells have big potential to capture a significant share of this expanding market owing to the rich reserves of raw materials, high performance and low prices. Preliminary life cycle assessments indicate that perovskite solar modules are anticipated to have a reduced environmental effect and a quicker energy payback time (EPBT) [25]. The increase in continuous running duration can significantly lower the maintenance and replacement costs of photovoltaic modules. Additionally, a number of research teams have estimated the LCOE and assessed the fabrication costs of PSC modules with various geometries. Following a thorough analysis that took into account the utilization of pricey metals (such as Ag and Au) and vacuum deposition processes, Egan *et al* calculated that the PSC's manufacturing costs range from \$87 to 140 m<sup>-2</sup>, with LCOE values from 9.0 to 18.6 cents kWh<sup>-1</sup>, which is comparable with commercial crystalline silicon and cadmium telluride solar cells. This anticipated cost will also be further decreased by using large-area preparation techniques like screen printing, R2R, affordable transport layers, or electrode materials [26]. Besides, their lightweight and flexible nature enable innovative designs and integration into various

surfaces, expanding their potential market reach. The versatility of perovskite solar cells makes them suitable for a wide range of applications, including rooftop solar panels, solar farms, portable electronics, and building-integrated photovoltaics. These characteristics will further add PSMs' commercial attractiveness and facilitate the realization of continuously large-scale preparation. At present, numerous research reports have focused on the scalable preparation methods of PSCs, like blade coating, slot-die printing, etc. With the research and technological innovation, the future of perovskite solar cell is promising.

## 3. Upscaling of perovskite photovoltaics

### 3.1. Scalable fabrication methods

Scalable manufacturing of efficient PSMs is critical for commercialization. And the key factor for this process is the fabrication of pinhole-free and homogeneous large-area perovskite film, which requires precisely optimized processing techniques (figure 3(a)). Up to date, the most explored technique for the highly efficient small-area PSCs is spin coating method due to the merit of depositing high-quality perovskite films with well-defined thicknesses and different compositions, laying a solid foundation for efficient PSMs with a certificated PCE of 22.87% (active area, 24.63 cm<sup>2</sup>) [27]. However, this method is limited to the substrate size and waste of 90% of perovskite ink, and is especially not applicable for the high throughput roll-to-roll (R2R) or sheet-to-sheet (S2S) manufacturing processes. Vacuum evaporation deposition method has shown the scalability for depositing perovskite films over 600 cm<sup>2</sup>, while the high expenses of large-scale vacuum equipment will hinder the further commercialization of perovskite

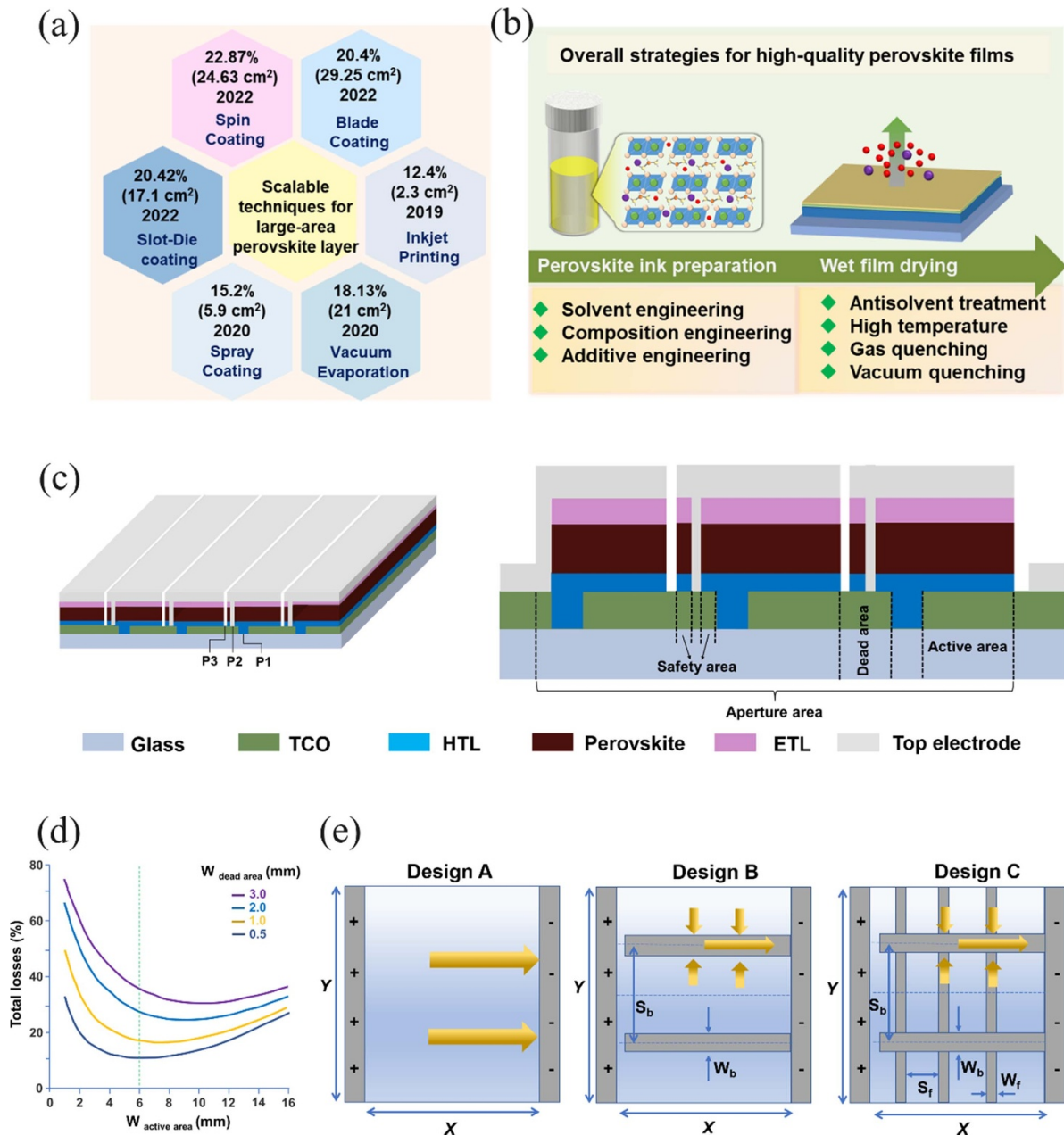


**Figure 3.** Fabrication method, structure design and advances of large-area perovskite solar modules. (a) Efficiency record of PSMs obtained by various deposition methods. (b) Advanced strategies for optimizing the quality of perovskite film. (c) The configuration and cross-section view of PSMs. (d) Illustration of the total power loss as function of the active-area width for modules with various dead-area widths. (e) Three cell designs. Design A: cell without metal grids; Design B: cell with parallel metal bus bars; Design C: cell with parallel metal bus bars and fingers, where gold arrows represent the direction of current flow through the front electrodes.

photovoltaics, leading to fewer reports of PSMs derived from this method [28].

From LCOE perspective, the scalable deposition methods should be low-cost and compatible with high throughput production processes (R2R, S2S). Therefore, blade coating, slot-die coating, inkjet printing, and spray coating, are more promising alternative techniques for scalable fabrication of perovskite films. Among those techniques, blade-coating is the most studied for preparing large-area perovskite films, leading to the current high PCE of 20.4% PSMs (active area,

29.25 cm<sup>2</sup>) [29]. However, this method also has limitations on the substrate size because the film thickness is gradually decreased along the coating direction due to the non-continuous ink supply, thus it is difficult to minimize the efficiency loss when the active area exceeds 30 cm<sup>2</sup>. Slot-die coating method works similarly to blade coating, but can overcome the thickness variation problem because the slot die head allows for continuous ink supply. Many reports with over 200 cm<sup>2</sup> area were derived from this method, giving it great potential in industrial production [6, 18, 30, 31]. The pro-

gress on PSMs based on the large-area film derived from inkjet printing, spray coating, and vacuum evaporation techniques are relatively slower (figure 3(a)) [32–35]. Inkjet printing is a non-contact manufacturing technology with the merit of preparing patterned perovskite film, but the inkjet inks usually require slow drying to achieve good processing stability and sufficient nozzle open times, which poses a great challenge in the film crystallization. Spray coating method can coat over a large-area perovskite film in a short time, but the ink droplets ejected from the nozzle usually have different sizes and can be easily overlapped on the substrate, affecting the final film thickness and crystal quality. To summarize, the slot die coating method will be the best candidate in the future scalable fabrication of PSMs.

Controlling nucleation and crystal growth is another key factor affecting the quality of large-area perovskite films. The perovskite ink preparation and the wet perovskite film drying are critical stages for precisely regulating the nucleation and crystal growth process (figures 3(a) and (b)). And the regulation of ink preparation can be divided into three perspectives: (a) solvent engineering, a strategy that utilizes solvents with different boiling points, surface energy, and donor number ( $D_N$ ) to control the solvent evaporation and crystallization; (b) composition engineering, a method that controls the composition of perovskite materials to regulate the band gap, stability, and crystallization of corresponding perovskite film; (c) additive engineering, a way that additives are used to adjust the perovskite nucleation and crystal growth during the film formation process. In addition, the drying process of wet films requires immediate supersaturation to accelerate heterogeneous nucleation, which is also very important to the final morphology and can be divided into antisolvent treatment, thermal annealing, gas quenching, and vacuum quenching. Among those additional treatments, gas quenching could be the most promising one due to the low equipment requirement, environmentally-friendly nature, no damage to the perovskite materials, and the compatibility with high throughput fabrication process.

### 3.2. Module design and process

**3.2.1. Fabrication process of modules.** The PCE of perovskite solar devices is decreased when enlarging the photoactive area, mainly originating from the resistive loss related to transparent conductive oxide (TCO). To reduce such losses, solar modules have been designed by interconnecting many small subcells either in series (monolithic modules) or in parallel [36–39]. Similar to silicon-based solar photovoltaics (PVs), the perovskite parallel solar modules can achieve a high photocurrent by accumulating photocurrent from the whole area (all subcells). However, parallel solar modules need a perfect photoactive area without any voids, because the existence of shunting paths will seriously reduce module's voltage, even probably to zero [40]. Thus, it is not popular to design parallel solar modules in thin film PVs. Here, we will give a brief review on the fabrication process of perovskite monolithic solar modules.

In comparison with small-area solar cell fabrication, module fabrication processes need extra laser or mechanical scribing steps to divide a large-area cell into desirable subcells with effective interconnections. Compared to the mechanical scribing method, the laser scribing process has been widely used to achieve high-quality and desirable line patterns, known as P1, P2 and P3 scribes. The P1 scribing lines are formed by scribing the back TCO-coated glass substrates (such as indium-doped tin oxide or fluorine-doped tin oxide). The goal of P1 scribing is to remove the TCO, and then form patterned subcells on a substrate. Before depositing the front electrodes, the P2 scribing process is generally conducted to expose the TCO. By doing so, the area of P2 scribing lines can be well filled by front electrodes to interconnect in series between two neighboring subcells. For an inverted PSM ( $p-i-n$ ) (figure 3(c)), the P2 scribes remove the electron transport layer (ETL), perovskite layer and hole transport layer (HTL). The traditional  $n-i-p$  solar module configuration can be built by only exchanging the position of two charge transport layers [41], with almost no changing of the scribing conditions. The P3 scribing process isolates the front electrode to separate neighboring subcells and achieve monolithic interconnections.

**3.2.2. Design of module structure.** The design of device structure is of vital importance to further enlarge the area of modules without sacrificing their efficiencies. After laser scribing P1, P2 and P3, some important parameters that determines its efficiency and stability should be noticed, i.e. safety area, dead area, active area and aperture area (figure 3(c)). As discussed earlier, the resistance-induced power loss ( $p_{Loss}$ ) decreases the efficiency of a module, which can be calculated using equations (1)–(3) [40, 42, 43]:

$$p_{Loss} = p_{Dead\ area} + p_{TCO} \quad (1)$$

$$p_{Dead\ area} = \frac{W_{Dead\ area}}{W_{Dead\ area} + W_{Active\ area}} \quad (2)$$

$$p_{TCO} = \frac{1}{3} \times R_{sh} \times \frac{J_{MPP}}{V_{MPP}} \times \frac{W_{Active\ area}^3}{W_{Active\ area} + W_{Dead\ area}} \quad (3)$$

where  $p_{Dead\ area}$  and  $p_{TCO}$  represent the dead area loss and TCO resistive;  $W_{Dead\ area}$  and  $W_{Active\ area}$  are the width of both areas;  $R_{sh}$ , and  $V_{MPP}$  are the sheet resistance of TCO, current density and voltage at maximum power point, respectively. Besides, geometry fill factor (GFF) is another important parameter that is defined as the ratio of the active area to the aperture area, which can effectively evaluate the performance of a module. Besides, the value of GFF remarkably affects aperture efficiency ( $\eta_a$ ). The GFF and  $\eta_a$  can be expressed by equations (4) and (5):

$$GFF = \frac{Active\ area}{Aperture\ area} \quad (4)$$

$$\eta_a = \frac{V_{oc} \times J_{sc}}{aperture\ area} \quad (5)$$



According to the above equations, it is important to maximize active area and minimize the dead area, but the module should have enough safety areas. Moon *et al* [42] simulates the relationship between the power loss ( $p_{\text{Loss}}$ ) and active area for various dead areas (figure 3(d)), further confirming the importance of the ratio of the active area and dead area. However, it is worth noting that P2 and P3 scribes should be wide enough to guarantee low contact resistance and further avoid shunting between neighboring subcells. Wilkinson *et al* [44] points out the importance of design of the front electrode grid to enhance the efficiency of large-area cells and modules (figure 3(e)). The parameters including cell width ( $X$ ), length ( $Y$ ), bus bar spacing ( $S_b$ ), bus bar width ( $W_b$ ), finger spacing ( $S_f$ ) and finger width ( $W_f$ ) remarkably influence the resistive loss of a module. For example, design A is widely used for small-area cells; a higher efficiency for an area  $>200 \text{ cm}^2$  was achieved from design C [45].

### 3.2.3. Characterization and assessment of modules.

Understanding the properties and defects of subcells and scribes in a module is of paramount importance to optimize the performance and reliability of PSMs. Except for common current-voltage curves, other characterization methods, such as optical microscope, Photoluminescence (PL), electroluminescence (EL), light-beam-induced current (LBIC) mapping, lock-in thermography (LIT), etc, have been widely used to investigate homogeneity or defects of modules [17, 38, 46, 47]. For example, the optical microscope is generally used to examine the quality and width of P1, P2 and P3 scribes. The PL and EL imaging provide important information about the distribution of local defects, charge recombination/transport obstacles related to impurities and non-uniformity. The high defect areas appear darker in the PL and EL images. The LBIC mapping gives information about photocurrent generation and distribution of a module, which significantly reveals the homogeneity of perovskite layers. Besides, the degradation mechanism of modules also can be investigated by the LBIC mapping [48].

### 3.3. Progresses and perspectives of PSMs

Up to date, the top-performing *n-i-p* PSMs were fabricated via spin-coating by Ding *et al* [27], which exhibited a best PCE of 22.87% with an active area of  $24.63 \text{ cm}^2$  (figure 4(a)). They used single-crystalline  $\text{TiO}_2$  rhombus-like nanoparticles as the ETL, which showed low lattice mismatch, high affinity with the perovskite layer, high electron mobility and lower defects density. Yoo *et al* combined the gas-quenching-assisted bar-coating method with solvent engineering using 2-methoxyethanol and *n*-cyclohexyl-2-pyrrolidone to obtain high-quality perovskite films, leading to PCE of 20.4% in  $29.25 \text{ cm}^2$  *n-i-p* PSMs (figure 4(b)) [29]. Bu *et al* used gas-quenching-assisted slot-die coating method to produce high-quality perovskite minimodules, (figure 4(c)) which showed PCE of 20.42% and 19.54% for an active area of 17.1 and  $65.0 \text{ cm}^2$ , respectively [36]. *N*-methyl-2-pyrrolidone (NMP) was added to the precursor to control the nucleation and

growth process of MA-free perovskite through facilitating the direct formation of  $\alpha$ -phase perovskite (figure 4(d)). It needs to mention that all the highly efficient *n-i-p* PSMs are based on doped Spiro-OMeTAD as the HTL, which suffers from the instability issue and high expense. As a result, developing cheap dopant-free HTLs is highly desirable. On the other hand, *p-i-n* PSMs with copper as the top electrode has great potential in obtaining stable and efficient PSMs [49–52]. But the PCE is relatively lower than that of the *n-i-p* PSMs. The highest PCE for *p-i-n* PSMs is 19.2% with an aperture area of  $50.0 \text{ cm}^2$ , fabricated by Chen *et al* via blade-coating method [49]. It was also noted that the voids caused by trapped DMSO at buried interface could deteriorate the device performance and should be properly handled (figure 4(e)). The performance of large-area *p-i-n* PSMs is yet to be improved to catch up with that of the *n-i-p* PSCs.

## 4. Stability of PSCs

### 4.1. Evaluation standards

Apart from the upscaling issue, another equally critical task is to boost the stability of PSCs. In practice, PSCs are subjected to external environmental stresses during operation, which degrade the PSCs from all aspects, i.e. encapsulation unit, electrodes, transport layers, interfaces, and perovskite films. This draws forth the development of standards to assess the stability of solar cells. Among the existing test and evaluation standards, IEC 61215, proposed by IEC, is the most-used industry standard today. It covers a range of detailed and continuous stress tests and provides accelerated aging conditions to evaluate the service life of solar cells under real-world use scenarios. As with mature PV technologies such as crystalline silicon and GaAs, passing IEC 61215 is the most fundamental precondition for the commercialization of PSCs. A series of tests evaluate the stability under stimuli of light, heat, ambient environment and mechanical impacts within the IEC 61215, the details of which have been elaborated by Holzhey and Saliba [53]. Official module testing for IEC 61215 standard follows the flowchart in figure 5, and main tests include 1-sun illumination ( $1000 \pm 100 \text{ W m}^{-2}$ ), UV-light ( $15 \text{ kW h m}^{-2}$  of UV irradiation between 280 and 400 nm), hot-spot ( $55^\circ\text{C} \pm 10^\circ\text{C}$ , under  $1000 \text{ W m}^{-2}$  irradiance with the maximum power dissipation), outdoor conditions (maximum power point (MPP) tracking at least  $60 \text{ kW h m}^{-2}$  of irradiation), damp heat ( $85^\circ\text{C}$  85% relative humidity (RH), 1000 h), thermal cycling ( $-40^\circ\text{C}$ – $85^\circ\text{C}$ , 200 circles), humidity freeze ( $-40^\circ\text{C}$ – $85^\circ\text{C}$ , 85% RH), hail impact (ice balls with a weight of 7.53 g and a speed of  $82.8 \text{ km h}^{-1}$ ) and mechanical load (at least 2400 Pa), etc.

### 4.2. Mechanism for instability under stresses

Currently, many reported PSCs have passed an individual test or several tests of IEC 61215 standard [7, 8, 54, 55], which largely inspires the whole PSCs community. However, for the real industrial requirement, the PSCs should work well at outdoor conditions for at least 25 years. To break through the

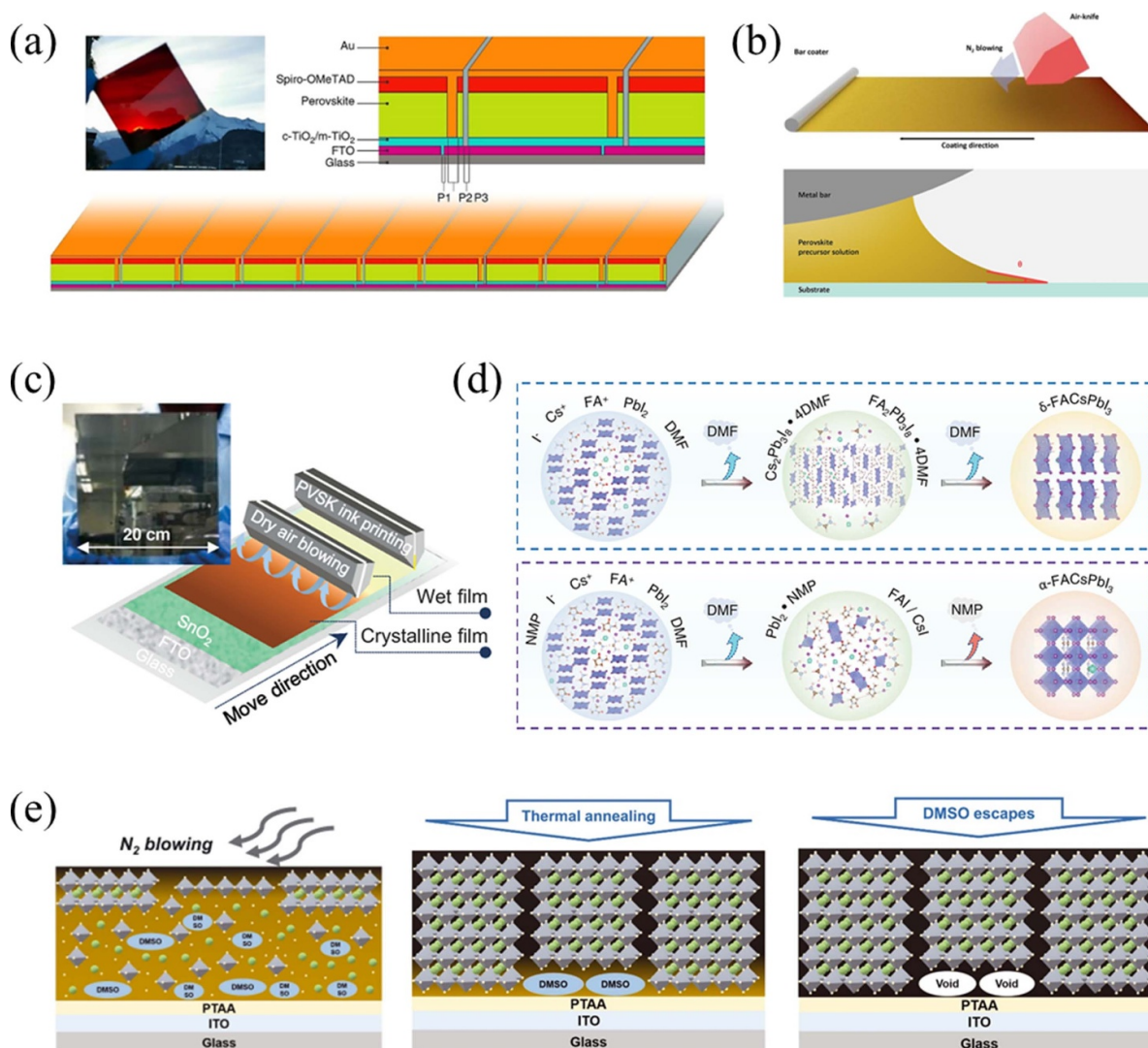


**Figure 4.** (a) Picture of the fabricated films and the schematic diagram of modules with 9 subcells in series. Reproduced from [27], with permission from Springer Nature. (b) Air-knife-assisted bar-coating and the sketch of precursor front. Reprinted from [29], © 2021 Elsevier Inc. (c) Slot-die printing with low-pressure dry air blowing. The inset is a picture of a  $20 \times 20 \text{ cm}^2$  perovskite film. (d) Illustration of crystal growth process with and without NMP. From [36]. Reprinted with permission from AAAS. (e) Illustration of the formation mechanism of voids at buried interface. From [49]. Reprinted with permission from AAAS.

instability bottleneck of PSC, it is imperative to reexamine the degradation mechanisms under each kind of stimulus, and find out how to control the manufacturing conditions to prevent it from degradation. In this regard, we review the mechanism for instability under most common external stresses, including light illumination, heat, ambient environment (moisture and oxygen), and radiation. The influence of each stimulus on the stability of PSCs are summarized in figure 6.

**4.2.1. Light illumination.** Commercial solar panels take advantage of the energy from sunlight, which covers the wavelength range from ultraviolet (UV) to near infrared (NIR). All the lights can affect the stability of our PSCs modules. Specifically, the UV light, with relatively high photon energy, challenges the stability of encapsulants due to the existence of unstable organic ligands such as ethylene-vinyl

acetate (EVA). In addition, this UV exposure is also harmful to the organic ligands within PSCs structure, like in the transport layers or perovskite layer. To avoid it, a practical strategy is to coat a down converting layer on top of PSCs where high-energy UV light is transformed into low-energy visible light [59]. Another possible solution is to use UV filter to prevent the penetration of UV light into PSCs.

With respect to the perovskite active layer or PSC itself, the sunlight influences the operational stability through two different aspects: (i) improving the performance and (ii) degrading the performance. The former one is mainly attributed to two different mechanisms: light soaking and light-induced lattice expansion (figure 6(a)). Light soaking is related to the phenomenon that device performance can be improved after continuous light illumination. It has long been discovered ever since the PCE of PSCs is at an initial stage (around 10%), where all the three key factors ( $V_{oc}$ ,  $J_{sc}$ , and  $FF$ ) as

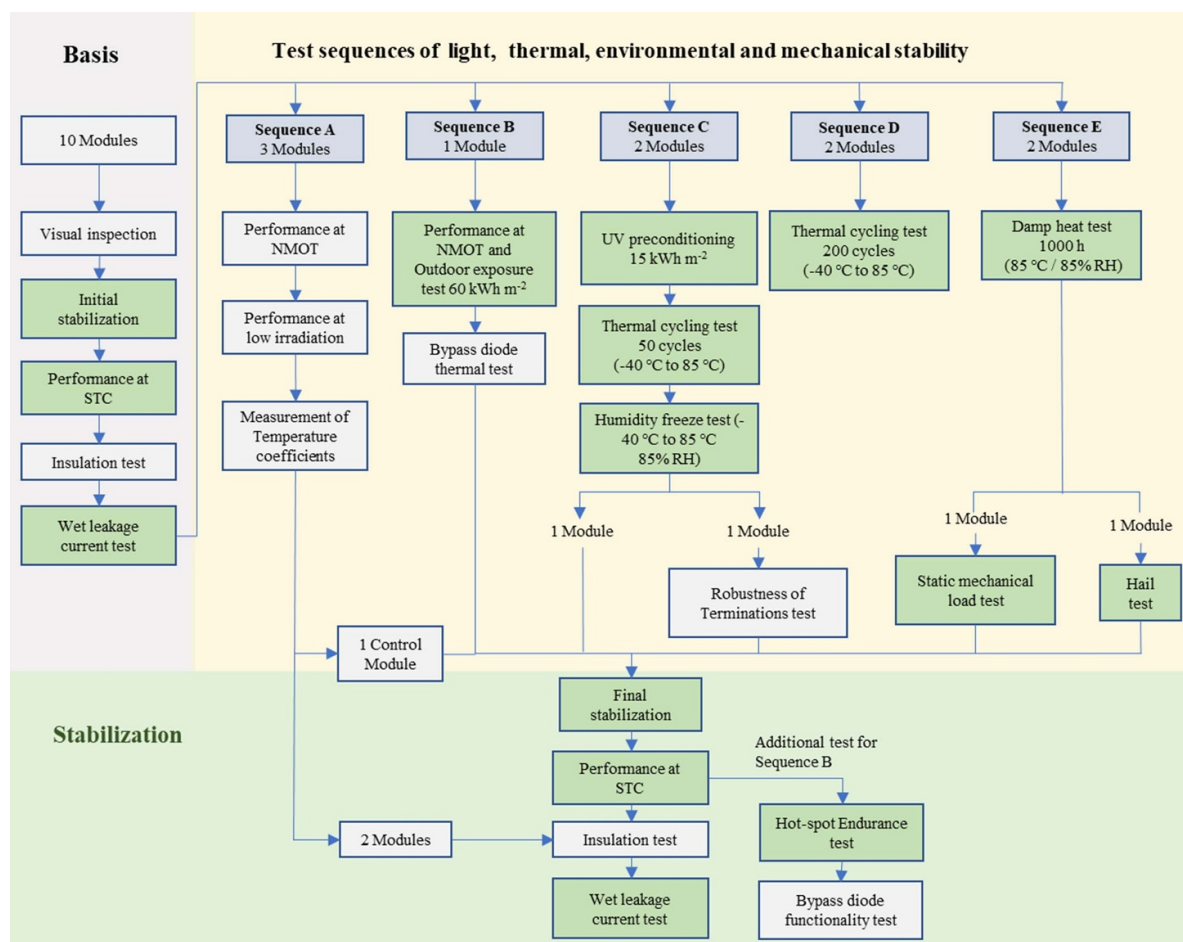


**Figure 5.** Flowchart of official PV module stability test for IEC 61 215 standard. Important stability tests for PSCs are marked in green. STC, standard test condition; NMOT, nominal module operating temperature. [53].

well as the  $J-V$  hysteresis can benefit from long-term light illumination. Through combined optoelectrical characterizations ( $J-V$ , impedance, photoluminescence, *etc.*), it has been acknowledged that the interfacial and/or bulk defects play the role [60, 61]. These defects serve as the non-radiative centers, leading to the drop of  $V_{oc}$ ,  $J_{sc}$ , and  $FF$ . Light illumination can heal these defects, and hence improve the device performance. Light-induced lattice expansion in PSCs was first reported by Tsai *et al* in 2018, where they found a uniform lattice expansion in mixed cations perovskite films after 180 min of exposure at one sun of illumination [56]. This expansion largely releases the perovskite strain, resulting in improved operational stability.

With continuous advancing device manufacturing techniques, the state-of-the-art perovskite films show much less light soaking effect or light-induced lattice expansion effect resulting from improved film quality. Alternatively, the light-induced degradation becomes the bottle-neck problem for PSCs stability. One of the key origins is the ion migration within perovskite layer, where halide anions or organic A site cations tend to migrate along the electric field. As a result, the photoelectrical properties of perovskite layers will be changed, hindering the intrinsic stability of PSCs modules.

Researchers attributed this unwanted phenomenon to surface defects dominated process [62] and/or strain-activated process [63], presenting two practical strategies to boosting PSCs stability. It should be pointed out that the ion migration process becomes more serious in mixed-halide perovskite systems, indicated by obvious phase separation issue. For instance, in the mixed Br/I perovskite film, Br-rich and I-rich domains tend to aggregate separately, leading to variation in PL spectrum and also the  $J-V$  characteristics [63]. Interestingly, Mao *et al* provided another new phenomenon that this light-induced phase separation can be reversible under sufficiently high illumination intensities [64]. The overall studies highlight the importance of improving PSCs stability via mitigating the light-induced ion migration processes.

There are also some parasitic factors caused by light illumination, such as heat and dark spots. When the PSCs panels work at high illumination intensities, their temperature will be very high, resulting in the thermal issue. Another case we need to consider is the existence of dark spots caused by fabrication imperfection or the dirt on the panels when setting up. These dark spots, acting as an electricity-consumption diodes, will generate more heat during operation and thus lead to more serious heat degradation issue.



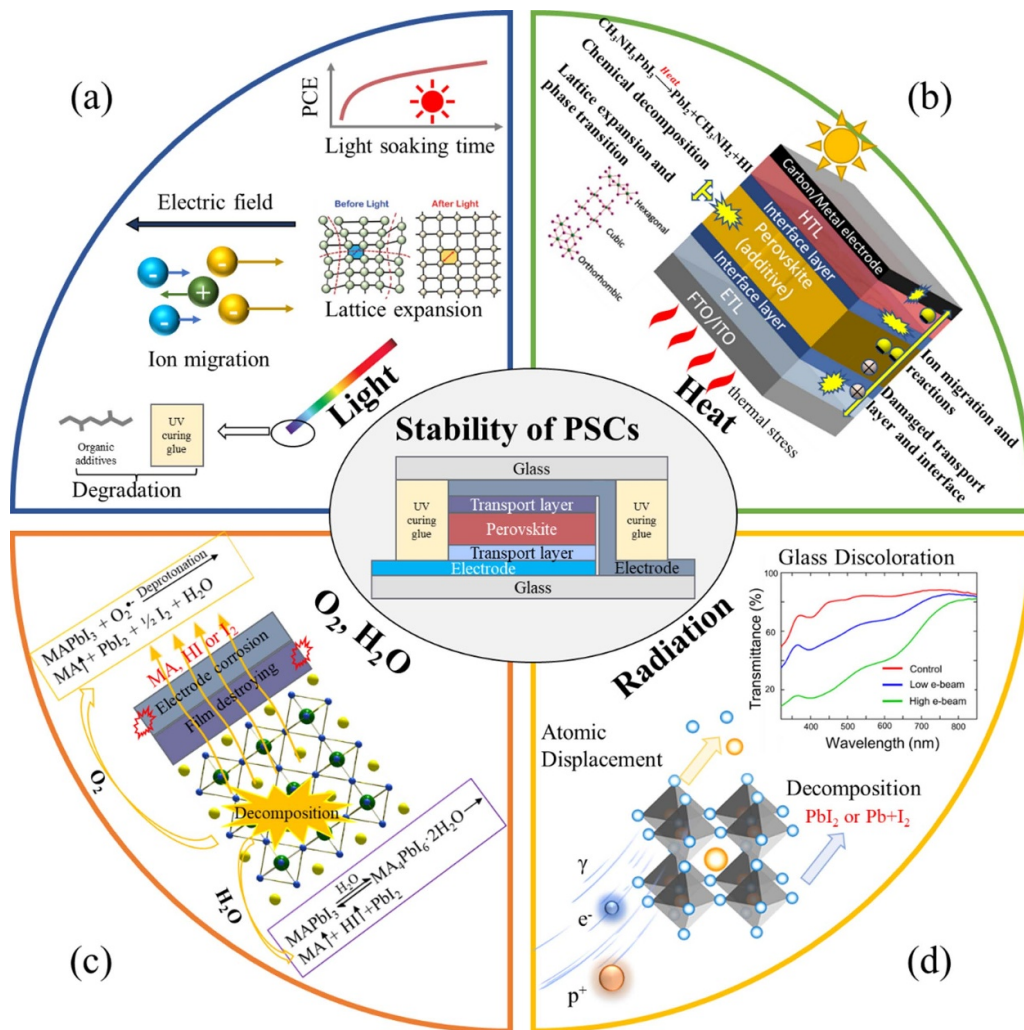


**Figure 6.** Schematic diagram to show the factors that influence the stability of PSCs: (a) light, (b) heat, (c) ambient environment and (d) radiation. Lattice expansion. From [56]. Reprinted with permission from AAAS. Lattice expansion and phase transition. Reprinted with permission from [57]. Copyright (2016) American Chemical Society. Glass discoloration. Reprinted with permission from [58]. Copyright (2020) American Chemical Society.

**4.2.2. Heat.** PSCs can be heated to high temperature after long-time light exposure. According to the IEC 61215 standards, the thermal stability is generally required to reach 85 °C, which is converted to 0.093 eV [65]. When maintained at 85 °C for 24 h in a nitrogen atmosphere, the MAPbI<sub>3</sub> will decompose into PbI<sub>2</sub> (CH<sub>3</sub>NH<sub>3</sub>PbI<sub>3</sub> → PbI<sub>2</sub> + CH<sub>3</sub>NH<sub>2</sub> + HI), which is due to the low formation energy of MAPbI<sub>3</sub> (0.11–0.13 eV) [66, 67]. The decomposition rate of MAPbI<sub>3</sub> will be faster at higher temperatures.

Several factors affect the thermal stability of PSCs jointly, as summarized in figure 6(b). The influence of temperature on the lattice structure and phase transition of perovskite has been widely acknowledged. The transition temperature from tetragonal to cubic phase of MAPbI<sub>3</sub> is reported to be 327 K [68], while the transition of CsPbI<sub>3</sub> from orthorhombic to cubic phase requires a high temperature of 634 K [69]. Different

types of perovskites have different characteristics of crystal structures, and subtle lattice expansion or distortion can cause changes in the structural stability of perovskite materials, which in turn affect their stability in thermal environments. Besides, the organic–inorganic hybrid halide perovskite has significant ionic properties and its low activation energy of ion migration affects the long-term stability of the material [70]. When the external environment imposes certain thermal stress, ion migration will become more severe, which in turn affects the stability of the perovskite layer and even enters the transport layer and electrode to cause damage [71, 72]. Furthermore, the transport layer (TL) within the PSCs device assumes the pivotal function of extracting and transporting carriers and forming ohmic contacts with the electrodes, and thus has great impacts on the PCE and stability. First, the nature of the transport layer material will determine its chemical stability when exposed to high-temperature environments,



which have an impact on the defect density, carrier transport at the PVSK/TL interface, and the quality of ohmic contacts. The thermal stress will accelerate the aging and damage process, bringing a series of problems such as damage to the transport layer material, severe ion migration of the device, reaction between the electrode and the migrating ions, and damage to the perovskite layer [73].

**4.2.3. Ambient environment.** Moisture and oxygen are the earliest factors that were founded to induce perovskite decomposition and have been widely studied in PSCs. For moisture, it will induce the hydration of perovskite first (take MAPbI<sub>3</sub> for example), and the hydration product will decompose to MA, HI and PbI<sub>2</sub> (figure 6(c)). On account of the volatile nature of MA and HI, such decomposition reaction will be continued until complete degradation. Since H<sub>2</sub>O merely works as an initiator, one H<sub>2</sub>O molecule will induce the complete decomposition of perovskite theoretically. In contrast, oxygen by itself will not induce perovskite decomposition. However, if in bias or illumination, oxygen will accept electrons from perovskite and form superoxide O<sub>2</sub><sup>-</sup>, which will attack perovskite and induces its deprotonation (figure 6(c)) [74]. Owing to the volatile and reactive nature of decomposition byproducts (MA, HI or I<sub>2</sub>), the transporting layers and even electrodes can also be degraded accompanied with perovskite decomposition. For example, MA or HI will penetrate [6,6]-phenyl-C61-butyric acid methyl ester (PCBM) and Spiro-OMeTAD transporting layer through cracks or pinhole in the film, thus degrading its transporting property. In addition, the I-related species (HI or I<sub>2</sub>) may also react with and corrode metal electrode, destroying its conductivity and reducing devices area. At last, from the point of environment, Pb leakage of perovskite devices is also an inevitable issue, taken the toxicity and partially soluble nature of PbI<sub>2</sub> byproduct in water (1.6 mM at 25 °C).

**4.2.4. Radiation.** Apart from terrestrial applications, photovoltaics are the mainstream power sources for satellites, spacecraft and space stations operating in the inner solar system. Perovskite solar cell has emerged as a promising space photovoltaic candidate, by virtue of the merit of an ultrahigh power-per-weight ratio, [75] excellent stowed packing efficiency and especially the low manufacturing cost [76]. The operational lifetime of PSCs has been increased to over a year [9] by unveiling the device instability channels under terrestrial stresses (i.e. illumination, heat, moisture, oxygen, etc). In view of space application, PSCs will face a series of space stresses including ultra-high vacuum (UHV), temperature extremes and especially cosmic radiations [77, 78]. The effect of vacuum and temperature extremes could be mitigated by device structure engineering [79] and encapsulation [80]. Cosmic radiations, on the other hand, are the most severe environmental threats, whose doses will constantly accumulate during the device service life and harm the long-term operational stability of PSCs [81]. Fortunately, preliminary results indicated that perovskite solar cells have higher radiation tolerance compared to state-of-the-art space-based photovoltaics. However, they are certainly not indestructible.

Cosmic radiation can be categorized into two groups, i.e. high energy particle irradiation (electrons, protons, alpha particles and neutrons) and electromagnetic radiation (x-rays and gamma rays), as shown in figure 6(d). Electrons, protons and alpha particles are the most prominent irradiation sources in the near-earth space orbits. The annual fluence of various charged particles increases in the sequence of alpha particles, protons and electrons, indicating an increased probability to interact with PSCs [82]. However, the displacement damage per particle follows a reverse sequence (alpha particle > protons > electrons) due to their effective mass. Miyazawa *et al*, reported that MAPbI<sub>3</sub>-based PSCs can withstand accumulated doses of up to 10<sup>16</sup> electrons (1 MeV) and 10<sup>15</sup> particles cm<sup>-2</sup> protons (50 KeV), which can completely destroy c-Si and GaAs-based solar cells [83]. Chen *et al*, demonstrated that MAPbI<sub>3</sub> is highly sensitive to electron beam exposure, leading to the rapid decomposition into the hexagonal PbI<sub>2</sub> [84]. Xiao *et al* revealed that knock-on-induced defect formation and heat-induced phase transformation are the two major failure pathways caused by electron irradiation [85]. The inconsistency may be originated from the different energy, fluence and dose of electrons exposed. Lang *et al*, showed that triplecation perovskites exhibited an impressive radiation hardness, even exceeding that of SiC. The proton irradiation leads to a transition of MA-escape-induced deep energy-level defects to shallow defects [86]. The PSCs maintained 95% of their initial efficiency upon irradiation of protons at an energy of 68 MeV and a total dose of 10<sup>12</sup> p cm<sup>-2</sup>. Stranks *et al*, indicated that perovskite/copper indium gallium selenide (CIGS) and all perovskite tandems are better space photovoltaics candidates compared to perovskite/silicon tandem due to superior proton radiation hardness [87, 88]. Neutrons are created when protons pass through the atmosphere at low earth orbit or spacecraft shielding. Rossi showed that flexible PSCs with benzothiadiazole-modified P3HT hole transport layers are more resilient than spiro-OMeTAD under fast Neutron irradiation (10 MeV, 10<sup>10</sup> p cm<sup>-2</sup>) [89]. In addition to the effect on perovskite absorbers, common glass substrates (e.g. soda-lime glass) become darkened after irradiation, causing significant loss in short circuit current (figure 6(d)) [58].

Electromagnetic radiations are high-energy photons with energy ranging from 100 eV to 100 keV for x-ray and greater than 100 keV for gamma-ray. Perovskites are not stable under X and gamma rays irradiation. Svanstrom *et al* reported that the decomposition of perovskite mainly follows two pathways under x-ray irradiation [90]. (I) The decomposition of the organic cation under radiation, resulting in the generation of degradation byproducts from the organic component and the breakdown of the perovskite framework. (II) Radiolysis of lead halide framework to produce halide salts, halogen gas, and metallic lead. The composition of perovskites is a determining factor. In the case of Cs<sub>0.17</sub>FA<sub>0.83</sub>PbI<sub>3</sub>, x-rays caused the degradation of FA<sup>+</sup>, resulting in the formation of PbI<sub>2</sub> without metallic lead. While in the case of CsPbBr<sub>3</sub>, the decomposition products are metallic Pb, CsBr and Br<sub>2</sub>. Boldyreva *et al* observed similar composition-dependent degradation pathways when perovskites with various compositions were subjected to gamma-ray irradiation. MAPbI<sub>3</sub> is more

radiation-tolerant due to its unique self-healing characteristics [91]. Besides, gamma rays promote phase segregation of mixed halide perovskite via the formation of I-rich and Br-rich domains [92]. By using specialized glass to eliminate color centers and suitable encapsulation, the gamma-ray induced degradation could be greatly mitigated [93].

#### 4.3. Strategies to stability enhancement

To solve the instability of the soft lattice features brought about by the low formation energy of perovskite under thermal stresses, an intrinsically stable perovskite composition is highly desirable. The MA escape is a fatal problem undermining the stability of MAPbI<sub>3</sub> PSCs. Replacing the smaller-sized MA organic cation (MA: 2.17 Å) with HC(NH<sub>2</sub>)<sub>2</sub><sup>+</sup> (FA: 2.53 Å) can result in a tolerance factor of 0.99 and avoid chemical decomposition under thermal stress [94]. The suitable bandgap of FAPbI<sub>3</sub> makes it a priority for current researchers, but the photoactive black phase is thermodynamically unstable at room temperature (RT) [95]. To solve this problem, researchers have tried many hybrid components around the main body of FAPbI<sub>3</sub> and studied the A-site, B-site, and X-site components separately to achieve optimized ones with high PCE and stability [96]. A-site components, such as CsMAFA, CsFA, and RbCsFAMA, all exhibited excellent film quality and significant thermal stability enhancement [97, 98]. The selection of X-site anions, in addition to improving film quality, is also critical for regulating crystal structure, lattice stress, and residual strain to improve thermal stability [99, 100]. Brabec *et al* screened photothermal-stable perovskite materials out of a composition matrix consisting of 160 kinds of commonly-used perovskite compositions using a high-throughput robotic system (figure 7(a)). The  $T_{80}$  lifetimes for 160 kinds of perovskite compositions were summarized in figure 7(b). It turned out that the mixed-cation mixed-halide perovskites with ~5 mol% Br, 10–20 mol% MA and ~5 mol% inorganic cations showed highest photothermal stability (figures 7(b) and (c)) [101]. This work has a directed significance to the selection of intrinsically stable perovskite composition.

The formation process of perovskite film also affects its quality and stability. Commonly, additive engineering in the precursor solution is an practical measure for defect passivation [102, 103], crystallization modulation [104–106] and perovskite phase stabilization [107–109] during the crystallization process. Considering grain boundaries are the main channels for moisture or oxygen penetration, non-radiative recombination and ion migration [110], it is crucial to enhance the film quality through better grain boundary modification [111, 112]. Li *et al* used TMTA additives that in-situ cross-linked at grain boundaries to block moisture penetration, realizing stable inverted PSCs with 92.3% retaining of initial efficiency after storing for 1000 h in air (relative humidity of 45–60%) [113]. Han *et al* used 5-ammoniumvaleric acid (5-AVA) iodide additives locating at the grain boundaries to prevent MAPbI<sub>3</sub> from decomposition (figure 8(a)), the printable

mesoscopic device passed the key IEC61215:2016 standards and operated at MPP for more than 9000 h of  $55 \pm 5$  °C with negligible decay (figure 8(b)) [7].

Due to the crystallization process, many dangling bonds exist at the surface of perovskite films, which will become defective sites for degradation and more susceptible to external environmental influences [114, 115]. Therefore, surface passivation (for both top and buried surface) to reduce defects while inhibiting ion migration is a feasible way to reinforce the stability of PSCs. There are several common methods for the choice of surface passivation: (1) organic layers that could interact with the underlying perovskite surface, represented by Lewis acids or bases [55, 116, 117]. Recently, Hagfeldt and his coworkers proposed a new sulfonium-based molecule to passivate the upper surface of the perovskite film and extensively reinforced the stability of PSC devices, which retained 99% of its initial performance after operating 4500 h at maximum power point tracking, yielding a theoretical  $T_{80}$  of over nine years under continuous 1-sun illumination [118]. (2) inorganic layers such as PbSO<sub>4</sub> and chlorinated graphene oxide, which possess stronger bonding ability, intrinsic stability, and the ability to block ion migration than organic layers [119–121]. In addition, inorganic capping layer also possess better water-resisting property. Yang *et al* stabilized perovskite surface using lead oxyalts and the resulted PSC retained 96.8% of its initial efficiency after MPP tracking for 1200 h in air with relative humidity of  $60 \pm 10\%$  [119]. (3) quasi-2D perovskite capping layer. Forming LD/3D heterojunction can reduce the defect density and enhance the moisture-resistance property owing to the hydrophobic nature of 2D perovskite [54, 122, 123]. Through the optimization of 2D capping layer, Azmi *et al* fabricated stable PSCs passing ‘double 85’ test (85 °C and 85% relative humidity) (figure 8(c)) [54].

The selection of charge transport layers is also crucial for determining the device stability. Inorganic transporting materials are generally more stable than organic ones and are usually adopted in the stability tests. For instance, You *et al* greatly improved the air stability of PSCs by using NiO<sub>x</sub> and ZnO nanoparticles as hole and electron transport layers respectively, retaining ~90% of initial efficiency after 60 d storage in air with humidity of 30–50% [124]. Han *et al* adopted p-doped Ni<sub>x</sub>Mg<sub>1-x</sub>O and n-doped TiO<sub>x</sub> as carriers transporting layer and only ~5% efficiency loss was obtained after storage in air for 7 d [125]. To further improve devices humidity stability, researchers started to introduce extra moisture blocking layer in PSCs, such as Bi metals [126], GO [120] and cross-linked polymer [127]. While the doped Spiro-OMeTAD is generally adopted in most high-performance *n-i-p* PSCs, which has an adverse impact on device stability on account of the water absorption of its conventional additive Li-TFSI and the holes left by the evaporation of TBP by heat [73]. Therefore, the development and use of stable, undoped organic [128–131] and inorganic [125, 132, 133] transport layer materials, or the dopants with good stability [134] is the leading way to solve the problem. Aiming to address the issue of electrode corrosion, Li *et al* intro-

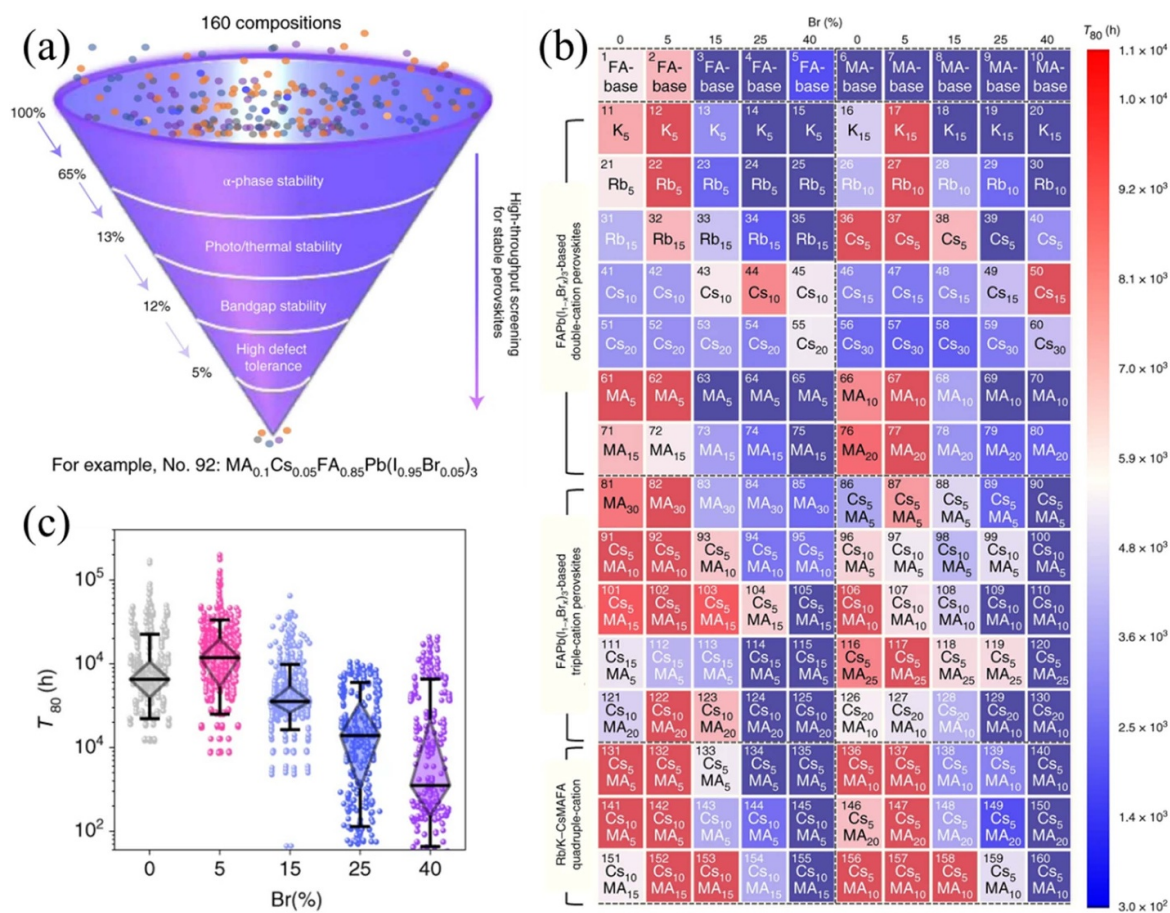


**Figure 7.** (a) The screening procedure for stable perovskite composition using the high-throughput screening system. The percentage point means the ratio passing the last round of screening. (b) The  $T_{80}$  lifetimes for the perovskites aged at 65 °C under 100 mW cm<sup>-2</sup> metal-halide light illumination in N<sub>2</sub>-filled atmosphere. (c)  $T_{80}$  lifetime statistics for mixed-cation perovskites with different Br concentrations. Reproduced from [101], with permission from Springer Nature.

duced chemical anti-corrosion strategy to suppress electrode reaction in PSCs by using organic anti-corrosion inhibitor of BTA [135].

Besides, interfacial modification between the transport layer and electrode by inserting interlayers can inhibit the ion migration and chemical reaction there. Li *et al* passivated the interfaces of *p-i-n* PSCs by inserting an interlayer of organometallic compound ferrocenyl-bis-thiophene-2-carboxylate (FcTc<sub>2</sub>) between perovskite and ETL, which reduced the surface trap states and enhanced interface binding (figure 8(d)) [55]. The resulting devices maintained >98% of their initial efficiency after 1500 h MPP tracing under continuous 1-sun illumination, and passed the damp heat test and thermal cycling test (figure 8(e)) [136, 137].

Moreover, building a device structure without a transport layer and or with a carbon electrode is an effective option to deal with the metal electrode induced degradation [138, 139]. The commonly used metal electrodes like gold and silver are susceptible to corrosion by the accumulated ions diffusing from perovskite layer and charge transporting layer, which compromises the overall stability of the device. Additionally, the diffusion of metal elements into the charge selective layer

and perovskite layer could result in the formation of metal halides, also undermining the stability of the device. By contrast, carbon electrode can greatly augment the stability of solar cells by virtue of its chemical inertness, hydrophobic properties, and the elimination of using hole transport layer [140]. Low cost, plentiful resource and low process complexity further add its commercial potential. The pioneering work on carbon-based HTL-free perovskite solar cells was introduced by Han and colleagues in 2013 with a PCE of 6.6% [141], using carbon black/graphite as contact electrodes. Subsequently, the substitution of metal electrodes with carbon electrodes has garnered significant interest. After a decade of investigating, advancements in the optimization of compositions, structures, manufacturing methods, interfacial connections, and device layouts have led to the gradual improvement of PCEs in carbon-based perovskite solar cells to surpass 22% [142–145]. Upscaling of carbon-based perovskite modules is also on the way of progressing [146]. Han and his coworkers reported a 12.87% PCE for high-temperature carbon-electrode modules with an active area of 60.08 cm<sup>2</sup> [147]. Moreover, carbon-based PSCs has showed superior operational durability of over 9000 h, surpassing the stability of metal-based



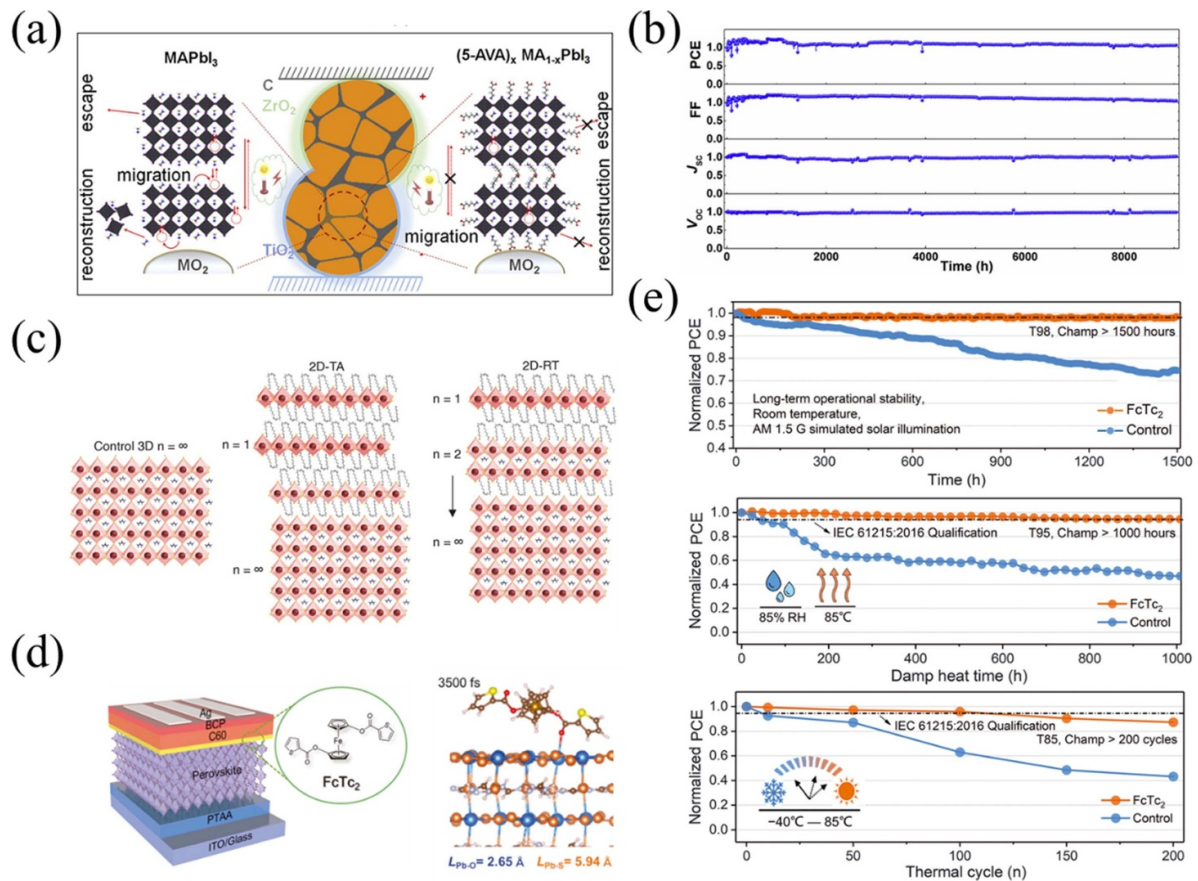


**Figure 8.** (a) The mechanism for 5-AVA enhancing the stability of MA-based PSCs. (b) Long-term MPP tracking for (5-AVA)<sub>x</sub>MA<sub>1-x</sub>PbI<sub>3</sub> PSC. Reprinted from [7], © 2020 Elsevier Inc. (c) Schematics of tailoring the 2D/3D heterostructure by tuning the annealing conditions. TA represents for thermal annealing at 100 °C, and RT represents for room-temperature process. From [54]. Reprinted with permission from AAAS. (d) Device structure of the inverted PSC with FcTc<sub>2</sub> as interface layer and the molecular dynamics simulations of the interaction between perovskite and FcTc<sub>2</sub>. (e) Stability tests including long-term operational stability under AM 1.5 G illumination, damp-heat test and thermal cycling test. From [55]. Reprinted with permission from AAAS.

devices [7]. These breakthroughs position carbon-based PSCs as a promising choice for achieving a balance between cost, efficiency, and stability among various types of perovskite solar cells, paving the way for a lucrative commercialization.

## 5. The toxicity of lead in PSCs

### 5.1. Concern about the lead toxicity issue

Pb is an essential element in high-performance perovskite solar cells, whose amount in the absorber is around 30 wt% (i.e. ~33.4 wt% in MAPbI<sub>3</sub>, ~32.7 wt% in FAPbI<sub>3</sub>, ~28.7 wt% in CsPbI<sub>3</sub>). Unfortunately, Pb is confirmed by the World Health Organization as a harmful substance to humans, especially for young children, because it can accumulate in the body and cause damage to multiple systems and organisms [148]. The effects of toxic Pb on human health have a long history. Babayigit *et al* reviewed the absorption, distribution, and excretion of Pb in humans when subjected to accidental Pb exposure [149]. There are three routes of ingestion of Pb, including gastrointestinal, respiratory, and dermal absorption

[150, 151]. Regardless of the way of ingestion, Pb compounds tend to transport throughout the body by the blood to soft tissues (liver, kidney, nerve tissue). Ultimately, 90% of the Pb is gradually accumulated in bone in the form of insoluble Pb phosphate, which has a typical half-life of 20–30 years. Pb causes damage to the human body by mimicking essential elements such as Ca, Zn, and Fe, leading to impaired enzyme and receptor function and heme activity interference. Pb is excreted through excretory mechanisms, including breast milk, making breastfed infants more susceptible to Pb poisoning. When exposed to MAPbI<sub>3</sub> perovskite, MAPbI<sub>3</sub> induces apoptotic cell death in human dopaminergic neuroblastoma cells (SH-SY5Y). It dramatically changes the proliferation capacity (e.g. increased size of cells, multiple nuclei, increased number of lamellar bodies) and mitochondrial activity (e.g. dramatically increased size, highly dilated intrapace, and severely damaged cristae organization) of the lung adenocarcinoma epithelial cells (A549) [152]. Pb is also harmful to ecosystems. When Pb<sup>2+</sup> from PSCs leaks into water, it causes zebrafish sac fry to suffer from growth inhibition, tail malformation, and spine deformity [153]. Moreover, Pb from



halide perovskites significantly increases Pb bioavailability in mint plants and causes mint plants to turn black, rot, and eventually die. Similar trends are observed in the case of chili and cabbage [154].

Although the lead content required and the Pb waste generated at the end of life in PSCs, according to relevant calculations, is far less than the amount produced by lead-acid batteries in 1 year [155], the potential Pb leakage risk from PSCs still needs to be avoided. To this end, countries worldwide have established a series of rigorous Pb content standards for drinking water and wastewater. For example, the Pb concentration of wastewater and drinking water in China should not exceed 1 part per million (ppm) [156] and 10 parts per billion (ppb) [157], respectively. The Pb concentration in drinking water in the United States should not exceed 15 ppb [158].

## 5.2. Strategies to prevent Pb leakage

In practical operation, perovskite solar panels may be damaged by outdoor natural factors (hailstones, hurricanes or fire, etc). Pb can leak from the damaged region with rainwater and contaminate the environment. Thus, it is imperative to develop effective strategies that reduce Pb leakage. In this section, we will briefly review some milestone works to gain insight into the eco-friendly operation of PSCs and provide helpful guidance to overcome the lead leakage issue further.

**5.2.1. Physical encapsulation strategies.** Physical encapsulation is extensively introduced to inhibit moisture and oxygen permeation, which are essential for addressing toxicity issues of PSCs. Physical encapsulation employs polymer and inorganic materials on the external surface of PSCs, which can effectively prevent physical damage-induced Pb leakage [159, 160].

Jiang *et al* [161] used the self-healing epoxy resin (ER) between the PSCs module and the encapsulation glass, which significantly slowed down the Pb leakage of the PSCs with no negative effect on PCE (figure 9(a)). The glass transition temperature ( $T_g$ ) of ER polymers is 42 °C, which can be easily reached by sunlight heating. When heated above  $T_g$ , the damaged encapsulation layer would heal and re-isolated the damaged device from the surrounding environment (figure 9(b)). In contrast to the device with the glass cover encapsulation, the device encapsulated with ER encapsulation reduced Pb leakage rates by 375 times, mainly ascribed to the self-healing characteristics and strong mechanical strength. Conings *et al* [162] reported that the devices with EVA/modules/EVA/glass architecture could leak little Pb in the fire safety assessment. However, lead leakage can only be slowed down by physical encapsulation and the toxic lead would still leak into the environment after long-term usage. Moreover, the additional glass substrates would increase the cost.

**5.2.2. Chemisorption strategies.** Chemisorption has been proven as more effective measure to prevent Pb leakage from damaged or broken perovskite solar cells or modules. This strategy captured  $Pb^{2+}$  ions by the firm chelate bonds between

the Pb ions and functional groups, including sulfate groups, thiols, and phosphate groups, when the Pb-containing constituent flows through Pb-adsorbing materials [167–170].

**5.2.2.1. Internal chemisorption strategies.** Chen *et al* [163] put forward a sulfonate groups-contained cation-exchange resin (CERs) to reduce the Pb leakage in PSCs (figure 9(c)). As a consequence, CERs combined with carbon electrodes and glass cover reduced the lead leakage by 62 times (figure 9(d)), down to 14.3 (ppb), which meets the US Federal 40 Code of Federal Regulations. Later, Chen *et al* [171] designed a mesoporous sulfonic acid as an insulating scaffold in PSCs to further reduced the amount of leaked Pb to 11.9 ppb in acidic water.

Wu *et al* [164] used 2D metal-organic frameworks (MOF) with free-standing thiol arrays to passivate the interface between the  $PC_{61}BM$  layer and the Ag electrode. The thiol groups in MOF can trap Pb ions by forming a water-insoluble Pb compound due to Pb-S bonds (figure 9(e)). As a result, the content of Pb leaked from damaged devices in the water soaking test was dropped down to below 20%. Recently, Xu *et al* [172] successfully introduced an in-situ cross-linked insoluble polymer (Spiro-NPU) as an internal encapsulating layer. The Spiro-NPU optimized the photovoltaic performance, yielding champion PCEs of 23.26% and 8 ppm of Pb leakage during 30 d.

Although the Pb-adsorbing additives and interfacial modifiers with certain thickness (~20–50 nm) could improve the performance and reduce the lead leakage, they could not completely block lead ions leaking from a typical ~500–1000 nm perovskite film [173]. In addition, the excessive additives could hamper the performance of PSCs and necessitate additional modification processes, such as spin coating and vapor-assisted process, will increase the cost.

**5.2.2.2. External chemisorption strategies.** External chemisorption strategies could isolate the device and ambient conditions to mitigate the Pb leakage. Specifically, Pb-adsorbing materials are deposited on the front and back sides of the device stack [174]. Li *et al* [165] integrated two Pb-sequestering materials, *P,P'*-di (2-ethylhexyl) methanedi-phosphonic acid (DMDP) and *N,N,N',N'*-ethyl enedia- mine-tetrakis (methylenephosphonic acid (EDTMP-PEO) on the glass and metal side, respectively (figure 9(f)), in which functional phosphonic acid groups can effectively absorb  $Pb^{2+}$  in rainwater. The DMDP film is insoluble in water, but has good water permeability. Therefore, when water penetrates into the device, it can effectively absorb  $Pb^{2+}$  in the water. As a result, the device with both sides coated with Pb-sequestering films exhibited 97.7% calculated sequestration efficiency on average in the water-soaking test (figure 9(g)). The above method requires additional spin coating process, which also complicates device fabrication.

To adapt the scalable and commercial fabrication of Pb-sequestering layer, Li *et al* [175] further designed a scotch-tape-like MDP-EVA package on both sides of devices with standard and inverted structures. During 3 month outdoor test,

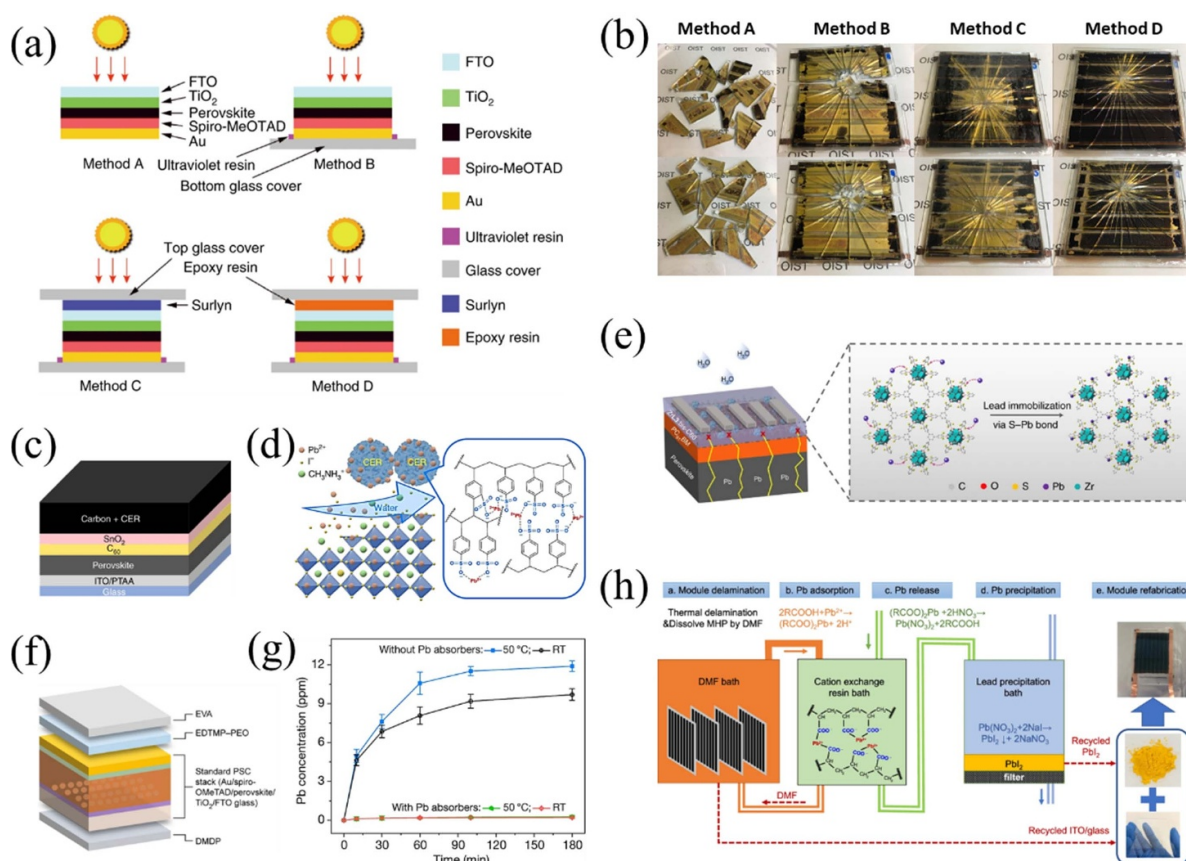


**Figure 9.** (a) Schematic of four encapsulation methods (b) Attacked perovskite solar modules with different encapsulation methods after the first water dripping test (top row), and after being heated at 45 °C for 4 h and the second water dripping test (bottom row). Reproduced from [161], with permission from Springer Nature. (c) Device structure for perovskite solar cell with CER encapsulation layer. (d) Schematic of Pb leakage prevention via CER. Reproduced from [163], with permission from Springer Nature. (e) Device structure of perovskite solar cells with 2D conjugated MOF as electron extraction layer and the proposed mechanism for Pb leakage prevention. Reproduced from [164], with permission from Springer Nature. (f) Device structure of perovskite solar cells with Pb absorbing materials DMDP and EDTMP-PEO on the front and back sides respectively. (g) Water soaking test for damaged PSCs with and without Pb-absorbing materials at RT and 50 °C respectively. Reproduced from [165], with permission from Springer Nature. (h) Roadmap for recycling perovskite solar modules. Reproduced from [166]. CC BY 4.0.

the Pb-absorbing tapes can seal more than 99% of the Pb ions in the PSCs, this tape can be easily applied to a variety of PSCs regardless of their equipment configuration. At the same time, this method is applicable to the general fabrication method of PSC encapsulation without affecting the device performance. However, repeated scraping on the EVA film tends to make the distribution of lead adsorption molecules uneven, resulting in poor batch reproducibility. More effective external chemisorption strategies with better batch reproducibility should be developed.

**5.2.3. Recycling and reusing of PSCs.** The costly and poisonous materials from the end-of-life PSCs could be recycled and reutilized in the manufacturing of new photovoltaic devices, which is of crucial significance for decreasing their environmental impact, saving costs on raw materials, and shortening the device's energy payback time [176, 177]. Recycling, as a sustainable and eco-friendly route, effectively lower the cost and energy consumption, improving the rivalrousness of PSCs. Park *et al* [178] used the Fe-decorated

hydroxyapatite (HAP/Fe) hollow composite to recycle  $\text{PbI}_2$  and  $\text{TiO}_2/\text{FTO}$  substrate. Later, they utilized recycled materials to fabricate PSCs and yielded a comparable PCE of about 18%. Similarly, Chen *et al* [166] utilized DMF and CER to dissolve the perovskite layer and recycle  $\text{PbI}_2$ , respectively. The detailed procedure for PSM recycling is shown in figure 9(h). The recycled  $\text{PbI}_2$  was used as the precursor material, achieving a comparable PCE of 20.4%. Furthermore, recycling materials including ITO glass, back cover glass, and raw perovskite could save  $\$4.24 \text{ m}^{-2}$ .

### 5.3. Towards commercialization

Nowadays, much research attention is paid to diminishing the environmental impact of PSCs. Considerable breakthroughs in the mitigation of Pb leakage during the device service life and recycling of Pb at the device end of life have been achieved. In view of perovskite solar cell commercialization, several measures could be taken, which may hold the key to further alleviating the environmental impact of PSCs below the threshold of Pb content standards and public acceptance.

Fast adsorption speed and large adsorption capacity are the keys to lead-trapping materials, either as encapsulants deposited externally or as additives integrated into PSCs. Besides, the lead-trapping materials need to have high selectivity in the presence of  $\text{Ca}^{2+}$ ,  $\text{Mg}^{2+}$ , which are common ions in rainwater. From this perspective, small molecules and polymers with functional groups that demonstrate strong binding energies with  $\text{Pb}^{2+}$  (e.g.  $-\text{PO}_3\text{H}_2$  and  $-\text{SO}_3\text{H}$ ) are ideal lead-trapping materials. In addition, the lead-trapping materials should have an ignorable influence on the performance of PSCs. This means that when used as an encapsulation layer on the glass side, it should not affect the light transmittance. And when used as a part of PSCs, it should not affect the carrier transport characteristics. Considering the aforementioned factors, advanced lead-trapping materials from a molecular engineering viewpoint should simultaneously realize multi-functions, such as anti-reflection, self-cleaning, and defect passivation. Other properties such as high robustness against environmental stimuli (UV irradiation, heat and moisture) and impact resistance are closely related to long-term reliability, which are also required. In view of technology commercialization, the lead-trapping materials should be cost-effective and reusable. The large-scale processability and industrial practicability should also be considered.

Regarding lead leak testing for PSCs, we should create specialized testing protocols. Simultaneously, it is essential to simplify methods of obtaining accurate data and develop mathematical models of lead leakage in order to mimic realistic meteorological conditions in computers. Integration of various encapsulation methods and recycling strategies to achieve lower cost, lower lead leakage and greater efficiency, as well as the development of testing standards, should be the focus of future study.

## 6. Encapsulation of PSMs

The instability of perovskites in the ambient environment (light, heat, and moisture) and their toxicity limits their development towards practical applications and commercialization. Encapsulation is a universal approach to enhance environmental stability and avoid the lead leakage caused by rainwater and physical damage. Compared to commercial silicon, perovskite devices have more stringent requirements in encapsulated strategies on account of the unique physicochemical properties of perovskite materials [179]. Materials chosen to encapsulate perovskite devices need to be chemically inert, resist to water and oxygen, have good toughness, and do not degrade perovskite. As a result, it is very important to investigate the most suitable encapsulation materials and strategies for metal halide perovskites.

### 6.1. Encapsulation materials

The original purpose of encapsulation is to greatly improve device stability by protecting them from ambient conditions.

Macromolecule materials can easily meet these characteristics and have low requirements for encapsulation technology. They can be simply coated onto the device to inhibit the erosion of ambient environment. Polydimethylsiloxane (PDMS) is a representative material that can be easily synthesized, which exhibits excellent hydrophobicity and ductility due to the existence of Si–O. Liu *et al* coated PDMS onto PSCs, greatly enhancing the stability to over 3000 h in the air [180]. Moreover, the properties of PDMS make it suitable to be applied in flexible perovskite devices as well [181]. Similar materials such as 1H,1H,2H,2H-perfluorodecyltrichlorosilane (FOTS) and adamantane have also been reported [182, 183]. In addition, Han and co-workers demonstrated that polyurethane (PU) or polyolefin (POE) is another great choice for encapsulation [184]. However, these materials require relatively high temperatures (80 °C or higher) to solidify or adhesion with devices, making them unsuitable for encapsulating all types of perovskite devices. Epoxy has been the most popular encapsulation material due to its strong water resistance and excellent adhesion. Flexible curing by heating or UV irradiation makes it suitable for almost all types of perovskite devices. Dong's group obtained stable PSCs at high temperature and relative humidity by simply covering the perovskite device with epoxy [185]. Unfortunately, epoxy is not suitable to direct contact with the perovskite device because its vapor and by-products formed during the process of UV-curing can cause great damage to the perovskite [186]. To avoid the negative effect of epoxy, Lidzey *et al*, introduced polyvinylpyrrolidone (PVP) as a protective interlayer between the perovskite devices and epoxy. They demonstrated that the PVP can further prevent water and oxide to form multilayer encapsulation for PSCs. The well-sealed device can maintain 80% of its initial performance under strong light irradiation after 1500 h [187]. Chen *et al* applied paraffin as a low-temperature encapsulant to modify epoxy, which has a great ability to eliminate residual water and oxygen. PSCs encapsulated with modified epoxy exhibited superior operational stability under continuous light irradiation over 1000 h [186]. Besides, other novel materials like graphene,  $\text{SiO}_2$ , or  $\text{NiO}$  have also been reported to be adopted in encapsulation [188–190]. However, simple encapsulation cannot guarantee the stability of perovskite devices to meet the commercialized standard.

### 6.2. Milestone works for encapsulation

In order to address the instability problem of PSCs, developing effective encapsulation strategies is as important as enhancing the intrinsic stability of the PSC devices themselves. In 2017, Baillie's team used polyisobutylene (PIB), which is a mature encapsulation material in CIGS solar cells, to encapsulate the PSCs via a blanket-seal method. They pointed out that heat is the major driving force for the degradation rather than moisture and PIB via blanket-seal can efficiently suppress the formation of by-products of perovskite to improve the lifetime of the device to 200 d under shelf life test [191].



After that, they found that the blanket-seal technology combining polymer and glass is extremely effective in preventing adverse decomposition reactions, enabling the PSCs to survive more than 1800 h and 75 cycles of humidity freeze test, which exceeded the requirement of IEC61215:2016 standard for the first time [8]. To date, more and more groups have prepared perovskite devices that can meet the IEC61215 standard by combining stable PSCs and encapsulation technology [192]. Very recently, stable all-inorganic PSCs reported by Zhao *et al* exhibited great potential for commercialization [193]. They introduced a 2D capper layer to stabilize the CsPbI<sub>3</sub> perovskite and encapsulated the device with multiple layers. Exciting operational stability under continuous light at different temperatures was achieved and the predicted life span is up to five years. Nevertheless, most of the encapsulation strategies are only available at the laboratory scale, with the repeatability and effectiveness seriously affected by individuals. Exploring encapsulation technology that is suitable for a larger scale is necessary to promote commercialization. Chemical vapor deposition (CVD) technology is a representative tool to deposit compact encapsulating films in perovskite devices and it has the potential to apply on large scale. Liu *et al* encapsulated a 22.4 cm<sup>2</sup> PSC module with parylene via CVD technology and the sealed module can continuously operate for 2000 h under AM 1.5 G light illumination [194]. Other technologies including atomic layer deposition (ALD) or plasma technology are also reported [183, 195, 196]. But the application of these technologies is still in its infancy and it is necessary to further enhance their influence in encapsulation technology. Finally, it is noticeable that all the devices that have achieved over 1000 h of the IEC 61215 stability test are encapsulated with the assistance of glass. The glass encapsulation sacrifices flexibility and stretchability, which significantly limits the application diversity of halide perovskites.

Device encapsulation is also a feasible strategy to reduce the detrimental effect of Pb toxicity, which contains physical encapsulation and chemisorption. The encapsulation method has the advantage of being universal and the ability to be used in various periods. Some polymers have self-healing properties when their glass transition temperatures ( $T_g$ ) are reached. For ER-based polymers, the  $T_g$  are even as low as 42 °C. In 2019, Jiang *et al* selected the ER (diglycidyl ether bisphenol A:octylamine:m-xylylenediamine = 4:2:1,  $T_g$  = 42 °C) as a encapsulant for PSCs [161]. The inserted ER layer between PSCs and the top glass cover could lower the Pb leakage rate by 99.7% under a simulated scene. Problems remaining with this method. For example, it may take a long time (several hours) to heal and it will fail when the environment temperature is close to its melting temperature. The other effective strategy is to utilize chemisorption to decrease lead leakage. The Pb-absorbing materials need to be insoluble in water but have good water permeability, and have functional groups in their molecules that can strongly bind with Pb<sup>2+</sup> ions so that they can effectively absorb Pb<sup>2+</sup> in rainwater. Besides, it also needs high transparency when it is applied to the light incident surface. Under these requirements, Li *et al* selected polar organic solvent soluble DMDP and deposited it on

the front glass side of PSCs by a solution coating process [165]. The functional group that adsorbs Pb<sup>2+</sup> ions is the phosphonic acid in each DMDP molecule, which reduces lead leakage by 96% in this structure. However, the metal ions from the rainwater or dust may lead Pb absorber to lose its functionality during long-term exposure. Thus, placing the Pb adsorber inside the encapsulation structure or underneath the perovskite layer should be a good option to avoid this issue [169, 171, 197].

Noted that the lead leakage strategies mentioned above are studied separately from the stability issues. The Pb absorbing materials cannot provide the same protection from physical damage as glass-based encapsulation solutions. As two equally important issues facing practical applications, seeking for synergistic solution is imperative but will greatly raise the complexity of the fabrication process. Therefore, Huang's group further presented a self-healable and lead-adsorbing ionogel-based encapsulation (poly-acrylic acid) strategy, which simultaneously improved impact resistance compared to pure glass encapsulation [198]. What's more, the self-healing ionogel is placed between encapsulation glass and the electrode, which can hold the shattered glass together even if the glass is completely broken. Finally, the encapsulated device passed the damp heat test (IEC 61215) and the lead leakage was effectively suppressed after the hail test. However, the temperature required for the self-healing process is higher than the normal working environment. As for the flexible and stretchable device, the hydrophobic tough self-healing polymer should be an ideal encapsulation choice. Different from most self-healing polymers, which are not suitable for stability improvement due to their substantial water vapor transmission rate, the hydrophobic tough self-healing polymer with dynamic multivalent hydrogen bonds and the low  $T_g$  enable self-healing without external stimuli. As a representative work, Kim's group tailored PDMS-MPU<sub>0.4</sub>-IU<sub>0.6</sub> hydrophobic tough self-healing polymer by incorporating strong hydrogen bonded 4,4'-methylenebis(phenylisocyanate) (MPU) and hydrophobic isophorone diisocyanate (IU) with PDMS [199]. By using it as encapsulation material, the broken polymer films can reconnect in ambient air or even in water, and the connected films have very good stretchability. The PDMS-MPU<sub>0.4</sub>-IU<sub>0.6</sub> polymer encapsulated device exhibited better lead leakage inhibition than the glass encapsulated device in cell viability test and over 1000 h of stability at 50 °C/50% RH condition.

## 7. Flexible perovskite solar cells and modules

With the innovation of portable electronic devices, wearable products gradually play an essential part in the emerging consumer level for electronic devices, which can be applied in biophysical behavior monitoring, human activity information recording, electrical vehicles or the IOT. Thus, as one of the core configurations in wearable devices, the exploration and attention on flexible power supply unit have scientific and practical significance. However, the continuous operation puts forward thorny requirements for



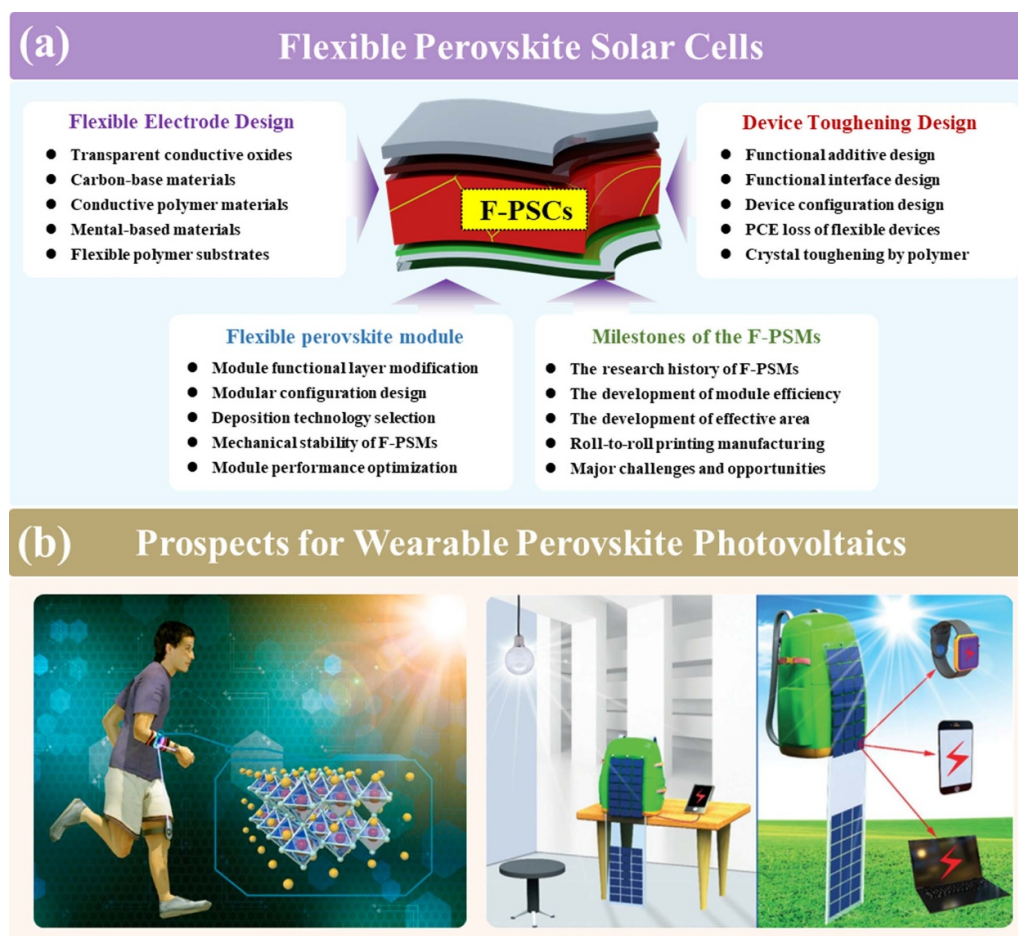


**Figure 10.** (a) Design strategy of flexible perovskite solar cells; (b) prospects for wearable perovskite photovoltaics [201]. John Wiley & Sons. © 2018 The Authors. Published by Wiley-VCH Verlag GmbH & Co. KGaA.

wearable devices. Using photovoltaic conversion technology as an external backup power source to reduce the battery capacity requirements may be an attractive strategy. Since the wet-processed PSCs are compatible with printing fabrication upon ultra-flexible substrates, the flexible perovskite modules are expected to meet the actual requirement of existing civilian portable equipment [200, 201]. However, the development of high-efficiency and stable large-scale flexible perovskite solar modules (F-PSM) still have a long way to go towards commercialization. Different from the rigid PSM, the requirement of F-PSM is much stricter, involving a flexible transparent substrate and a low-temperature process. It is also more complicated compared to their small cell counterparts, which not only needs to ensure the homogeneity of each function layer over a large area, but also needs to reduce the sheet resistance during the series connection between individual solar cells. To ensure the superior photovoltaic properties of F-PSM for commercial application, the manufacturing process should be critically designed and optimized (figure 10(a)). Despite great challenges it may encounter, F-PSM still enjoy huge commercial prospects owing to their great potential to be use as portable power sources in wearable electronics. (figure 10(b)). In this section, we have summarized the feasible selection of electrode materials, substrates for F-PSCs, the toughening strategy

of each functional material, and the modular manufacture of F-PSMs.

### 7.1. Flexible electrodes

Flexible transparent electrodes are critical for F-PSCs. In order to obtain an excellent performance for flexible device, the flexible transparent electrodes should simultaneously possess high optical transmittance, low electrical resistance, superior flexibility and excellent conductivity. Previous significant researches have already demonstrated that TCOs, carbon-based materials, conductive polymer and metal-based materials are promising candidates in achieving highly efficient and stable flexible devices [202–204]. The basic performance parameters of commonly used flexible transparent electrodes are summarized in table 4.

**7.1.1. Transparent conductive oxides.** The TCOs play a pivotal role in the rapid and noticeable development of flexible transparent electrodes, including tin-doped indium oxide (ITO), fluorine doped tin oxide (FTO), aluminum doped zinc oxide (AZO), indium zinc oxide (IZO) and tungsten doped tin

**Table 4.** Summary of flexible transparent electrodes.

Electrode	Sheet resistance ( $\Omega \text{ sq}^{-1}$ )	Optical transmittance (%)	Bending properties	References
ITO	10–15	85–90	Medium	Kumar and Zhou [205]
AZO	<10	>85	Good	Mutiari <i>et al</i> [206]
IZO	<10	>90	Medium	Lee <i>et al</i> [207]
IWO	~35	>95	Good	Kim <i>et al</i> [208]
CNT	150–500	70–90	Good	Zhang <i>et al</i> [209]
Graphene	110–780	70–95	Good	Wang <i>et al</i> [210]
PEDOT:PSS	15–250	>80	Good	Lee <i>et al</i> [211] Worfolk <i>et al</i> [212]
Metal nanowire	1–25	>90	Good	Chen <i>et al</i> [213]
Metal mesh	<2	>84	Good	Zhang <i>et al</i> [214]
UTMFs	<10	>82	Good	Li <i>et al</i> [215]

oxide (IWO). Polymers coated with TCO have been commercialized and are the most popular flexible substrates to fabricate flexible devices. It is widely known that FTO is deposited at too high temperature, which renders its application impractical for polymer substrates. The manufacturing temperature of IZO is much lower than that of FTO, while ITO, AZO and IWO can be deposited at room temperature. AZO-based flexible devices could display a chemical interaction between AZO and perovskite, which dramatically deteriorates device performances [216]. ITO is the most frequently adopted TCO electrode and remains predominance in the flexible devices, which can be attributed to low-temperature fabrication process, high optical transparency and mature industrial manufacturing process. Up to date, the highest performance of F-PSCs is mainly achieved based on ITO/polymer electrodes. However, there are still serious issues when ITO electrode is applied in the latest-generation flexible photovoltaic devices. (I) ITO encounters the intrinsic brittleness obstacle. (II) The low abundance of indium resources and expensive vacuum deposition techniques would greatly increase the cost of production and make it less competitive compared with other transparent electrodes matched to roll-to-roll printing, restraining the potential for industrial manufacturing. (III) ITO prepared by current sputtering exhibits amorphous structures and rough surfaces, resulting in poor transparency and high sheet resistance. (IV) ITO is sensitive to acid and basis environments. These restrictions related to ITO are the insurmountable bottlenecks of commercializing flexible devices to satisfy the demand of an industrial protocol.

**7.1.2. Carbon-base materials.** Carbon-based materials like carbon nanotubes (CNTs) and graphene have been explored to be alternatives of the transparent electrodes due to their rich carbon composition, outstanding electrical properties, environmental robustness, flexibility, and direct scalable manufacturing capability. CNTs is a kind of unique cylindrical structured materials with nanometer diameter, which can be synthesized via floating catalyst CVD with good reproducibility. However, CNTs are difficult to be evenly dispersed, and their high sheet resistance and high roughness would weaken the carrier mobility and shorten the lifetime of flexible devices [217]. Therefore, a suitable method is needed to develop CNT

films with high conductivity and transparent via mass production. Compared with CNTs, graphene with single atom thickness is smoother, more conductive and more transparent in a broad wavelength range. Graphene possesses well chemical and mechanical stability, which is synthesized on platinum, copper or nickel foils through CVD and then transferred to the target substrate, resulting in lower reproducibility. Graphene has unstable carrier mobility, which is usually much lower than the theoretical value on account of the unsatisfactory quality of graphene film. As a result of the physical transfer process and the absence of chemical bonds, the weak adhesion between graphene and substrate could lead to inadequate contact and mechanical deformation during the bending process [218].

**7.1.3. Conductive polymer.** In order to break through the bendability limitation of ITO electrodes, conductive polymer is developed as a favorable alternative. With its solution processability, high optical transmittance, flexibility, and stretchability, PEDOT:PSS is well-suited for low-cost roll-to-roll industrial manufacturing. However, the inferior conductivity of original PEDOT:PSS film is the key challenge, which can be remarkably increased through the inclusion of polar solvents, elastomers, acids, and ionic liquids [219–221]. The acid-free strategy combined with polar solvent and post-treatment can effectively enhance the conductivity of PEDOT:PSS, which can be ascribed to the interconnected PEDOT:PSS and the separated PSS. Although the tunable work function enable PEDOT:PSS to be both cathode and anode, fewer studies have used it as the top electrode due to its potential to damage the the underlayer of perovskite film. Furthermore, PEDOT:PSS film is unstable under the stimuli of UV light, high temperature and moisture, which hinders its potential applications.

**7.1.4. Metal-based materials.** Considering the good conductivity and extensive optical transparency, metal-based electrodes in the form of metal nanowires, metal meshes and ultrathin metal films (UTMFs) are powerful candidates of electrodes in flexible optoelectronics. Metal nanowires, especially silver nanowires (AgNWs) have been esteemed the most promising metal nanowires because of their outstanding optoelectronic and mechanical properties. The main concern of

**Table 5.** Properties of flexible polymer substrates.

Substrate	$T_g$ (°C)	$T_m$ (°C)	Density (g cm <sup>-3</sup> )	Water absorption	Dielectric coefficient	Solvent resistance	Dimensional stability
PET	70–110	115–258	1.39	0.4–0.6	3.0–3.8	Good	Good
PEN	120–155	269	1.36	0.2	—	Good	Good
PI	155–270	250–452	1.36–1.43	1.3–3.0	3.4	Good	Fair
PDMS	–125	–43	1.03	>0.1	2.7	Good	Good
PES	225	315–335	1.37	0.43	3.5	Good	Good
PC	150	267	1.2	0.4	3.0–3.2	Poor	Fair

$T_g$ : glass-transition temperature;  $T_m$ : melting temperature.

AgNWs includes poor chemical stability, rough surface, high contact resistance, and loose adhesion of AgNWs on the polymer substrates. By adding additional materials or adopting novel preparation processes, these shortcomings of AgNWs electrode can be improved effectively [222]. Metal meshes including Ag, Pt, Au, Mo, Cu, Ni, and even hybrid meshes can be integrated with additional transparent conductive materials to conduct high-performance compound electrodes. Metal meshes prepared by photolithography method are expensive and time-consuming, primarily by evaporating the metal films on patterned photoresist film that is selectively exposed with a mask, and then peeling the photoresist. Novel manufacturing tactics for flexible devices with metal mesh electrodes need to be exploited to extend scalable fabrication. In addition, ULMFs with a thickness of around 10 nm are promising transparent electrodes. The application of ULMFs electrode in flexible devices is still restricted mainly owing to the lower light transmittance.

## 7.2. Flexible substrates

Flexible polymer substrates, such as polyethylene terephthalate (PET), polyethylene 2,6-naphthalate (PEN) and polyimide (PI), are the most prevalent and competitive flexible substrates by virtue of their high transparency, robust bendability, light weight, low cost and potential for roll-to-roll process. Although PET materials have been normally chosen as commercially flexible substrates for devices, their low heat resistance and mechanical stability are still inadequate for specific applications. Among these ideal flexible polymer substrates, PEN and PI are very attractive for high temperature tolerance, considering that most of the processing temperature of charge transport layer and perovskite films are more than 150 °C. The price of colorless PI is quite expensive. Polycarbonate (PC) and polyethersulfone (PES) exhibit outstanding optical transparency, which is conducive to substrate material of flexible photovoltaic devices. But the chemical stability of PC lags far behind other flexible polymer substrates. Additionally, flexible polymer substrates show poor permeability to oxygen and water molecules, and cannot completely prevent the attack from oxygen and water. Therefore, in order to realize long-term stability of flexible devices, more stable encapsulation approaches are urgently required. The properties of flexible polymer substrates are summarized in table 5.

## 7.3. Toughening strategies for F-PSCs

The mechanical stability of perovskite layer, charge transport layers, and the interfaces between them are the key to realize high-performance F-PSCs. In PSCs, the photoactive perovskite layer plays a decisive role to the efficiency. Therefore, improving the toughness of perovskite layer comes the first priority. To enhance the bendability of perovskite films, Chen *et al* incorporated an elastomer PU into perovskite precursor solution to crosslink the grain boundaries and formed a PU network in perovskite films, significantly improving the bendability and enhancing the crystallinity of F-PSCs [223, 224]. Using the similar PU polymer, Lan *et al* demonstrated that self-healing protection is also a feasible measure to reinforce the bendability of perovskite thin films [225]. Additionally, other crosslinking agents like methyl methacrylate and 5-aminovaleric acid have also been developed and applied to toughen mechanical stability of F-PSCs [226–228]. For example, Jiang *et al* incorporated a crosslinking oligomer of trimethylolpropane ethoxylate triacrylate (TET) into perovskite films and simultaneously improved the PCE and stability of the F-PSC [228]. Specifically, The TET-incorporated PSCs retained about 87% of its original value after 20 000 bending cycles at a radius of 4 mm. Besides, elastic encapsulating has also been reported to be an effective technique for improving the bendability of PSCs [229]. In addition, it is also important to develop high toughness ETL and HTL to further increase the mechanical stability of F-PSCs [230–232]. Recent works demonstrated that ETL [233] and HTL [234] with high toughness can substantially relaxes the mechanical constraint of the PSCs even under large bending deformation.

When the PSC is bent, partial PCE loss could be ascribed to the brittleness and discrepancy of perovskite thin film on different substrates. Inspired by the robust crystallization and flexibility of vertebrae, Meng *et al* implemented an interfacial layer made of conductive and glued polymer of PEDOT:EVA between the ITO and perovskite layer (figure 11(a)), which simultaneously facilitated directed crystallization of perovskite and improved the mechanical stability of the whole solar cell. An efficiency of 19.87% for 1.01 cm<sup>2</sup> F-SCs and an efficiency of 17.5% for 31.2 cm<sup>2</sup> PSMs were achieved [235]. The fabricated PSMs can work as wearable power sources for low-power devices (figure 11(b)). Increasing the adhesion toughness at the interface between



ETL and the perovskite layer is another strategy to enhance mechanical reliability of the F-PSCs. Padture *et al* introduced an iodine-terminated self-assembled monolayer (I-SAM) at the ETL/perovskite interface, successfully promoted the PCE of flexible PSC from 20.2% to 21.4%, and further improved its operational stability [236, 237]. We believed that when the bendability of all functional layers and interfacial adhesion in the F-PSCs are effectively improved simultaneously, the efficiency and stability of F-PSCs can be further enhanced.

#### 7.4. Flexible perovskite solar modules

**7.4.1. Materials and structure design.** Due to the unique requirements of large-scale F-PSMs, the materials and structure of devices should be seriously designed. Regarding the transparent conductive electrode, it normally consists of a plastic substrate (e.g. PET, PEN) and metal-oxide conductive thin films (especially the ITO). Given the fragility of ITO, it is hard to ensure mechanical robustness in the long term or under extreme bending. To solve this problem, alternative polymer conductive layer would be a better choice, which is also compatible with scalable deposition methods. Hu *et al* reported a slot-die printed large-scale polymer network electrode to replace the ITO on the PET flexible substrate in 2019, demonstrating a 10.9% efficiency with an aperture-area of 25 cm<sup>2</sup> and an 80% efficiency retention even after 5000 bending cycles at a curvature radius of 3 mm [219]. Given the poor thermal tolerance of flexible plastic substrates, the subsequent deposition of ETL/HTL should be controlled under a low temperature. Therefore, a lot of low-temperature processed nanocrystal films have been explored as the charge transport materials for F-PSMs, such as TiO<sub>2</sub>, SnO<sub>2</sub>, NiO<sub>x</sub>, [240, 241] *etc.* How to deposit the functional layers in a large scale is the main concern of F-PSMs. Table 6 summarizes the typical upscaling methods of each functional layer in F-PSMs. Upscaling deposition tools including printing, spray coating, or vacuum deposition have been developed to deposit large-scale charge transport layers efficiently [240, 242, 243]. However, the deposition of high-quality large-area perovskite films is always a major challenge even in rigid PSMs. Many efforts have been devoted to upscaling high-quality large-scale perovskite films, e.g. slot-die coating [241], blade coating [244], vacuum deposition [243], *etc.* And among them, solution processing methods are promising because of the compatibility with roll-to-roll (R2R) gravure-printing for mass production of F-PSMs [241, 245].

**7.4.2. Milestones of the F-PSMs.** The first F-PSM was reported in 2015 by Giacomo *et al*, which adopted a normal structure with mesoporous TiO<sub>2</sub> scaffold on an ALD-TiO<sub>2</sub> surface to enable efficiency of 3.1% on a 5.6 cm × 5.6 cm PET/ITO substrate [248]. And then in 2016, Yeo *et al* reported an invert structured F-PSM with a higher efficiency of 8.1% on an active area of 10 cm<sup>2</sup> by employing a molecular-doped reduced graphene oxide with fluorine atoms (MFGO) as the HTL on a PEN/ITO substrate [249]. To further increase the performance of F-PSMs, the layout of PSCs in a large-scale F-PSM should be carefully designed. An effective way is to

utilize laser scribing to replace mechanical scribing, which can not only improve the GFF but also reduce damage to the layer underneath [242]. In 2017, Dagar *et al* fabricated a fully laser-patterned formal structured FPSM with a PCE of 8.8% (active area of 12 cm<sup>2</sup>) by applying a mesoporous TiO<sub>2</sub> scaffold layer over a compact SnO<sub>2</sub> layer on PET/ITO substrate [250], and this is the first time a complete three-step laser scribing procedure (P1, P2, P3) was used in the manufacturing of F-PSMs.

Since then, the exploration for F-PSMs seems to have been ignited, including selecting different substrates [52, 216] and developing ultra-thin or wearable devices [235, 251]. Works have been done on seeking strategies to further improve the efficiency and stability of F-PSMs simultaneously, such as interface engineering or additive engineering of function layers [252]. For example, Bu *et al* developed a universal interface passivation strategy to improve the efficiency and stability of F-PSM by using potassium ions to treat the surface of a slot-die printed SnO<sub>2</sub> layer on PET/ITO substrate in 2018, as shown in figure 11(c) [238]. High efficiency of over 15% was achieved for an F-PSM on a large area of 16.07 cm<sup>2</sup>, as well as a good mechanical stability and no more than 30% loss even after 1800 bending cycles. In 2019, Hu *et al* reported a biomimetic crystallization of perovskite with the assistance of additives and a certified efficiency of 7.91% was achieved for a 56.02 cm<sup>2</sup> wearable F-PSM with a PEDOT:PSS/PDMS substrate [251]. And Dai *et al* reported a record aperture efficiency of 15.86% with an area of 42.9 cm<sup>2</sup> on flexible Corning Willow Glass using ammonium chloride (NH<sub>4</sub>Cl) additive in 2019 [52]. These excellent preliminary explorations broaden the potential of F-PSMs towards diverse application fields.

However, all these infusive achievements of F-PSM are based on a mini-module scale (<100 cm<sup>2</sup>), it is necessary to demonstrate the sub-module scale (>200 cm<sup>2</sup>) FPSM to break the upscaling limit. Chung *et al* firstly demonstrated large-scale flexible perovskite solar sub-modules through structure optimization in 2020 [253]. They reported a porous planar (Zn<sub>2</sub>SnO<sub>4</sub>/SnO<sub>2</sub>) ETL and demonstrated PCE of 12.9% and 11.8% for 225 cm<sup>2</sup> and 400 cm<sup>2</sup> aperture area respectively. Nevertheless, all the steps from ETL to HTL are based on a spin-coating method which is not an effective route for industrial manufacturing. Kim *et al* in 2020 [239] demonstrated a fully R2R printed PSC (figure 11(d)) with an efficiency of over 13%, the printing process of which is illustrated in figure 11(e). But it was based on small-area device, and fabricating large-area F-PSMs through scalable methods for all functional layers is still challenging. The advances for F-PSMs via scalable fabrication methods for all functional layers are summarized in table 6. There is still a long way to go towards commercialization for F-PSMs.

In addition, the flexible two-terminal (2T) perovskite/perovskite tandem solar cells [254] and 4T perovskite-Cu(In,Ga)Se<sub>2</sub> tandem mini-module [255] have also been developed in 2022. Tan *et al* enhanced the contact between NiO and perovskite through inserting a self-assembled monolayer. 23.5% efficiency was achieved for a 1.05 cm<sup>2</sup> flexible all-perovskite tandem solar cell. Theoretically, it would have a higher performance, and its development will further accelerate the commercialization of F-PSMs.



**Table 6.** Advances of F-PSMs via scalable fabrication methods (none spin-coating).

Year	Structure	Materials choice and fabrication methods						PCE (%)	References
		Bottom electrode	ETL	Perovskite	HTL	Top electrode	Area (cm <sup>2</sup> )		
2015	PET/ITO/ZnO/Perovskite/P3HT/Ag	PET/ITO (commercial)	ZnO (slot-die coating)	Sequential roll-to-roll	P3HT (slot-die coating)	Ag (evaporation)	40	~1	Hwang <i>et al</i> [245]
2019	MgF <sub>2</sub> /Willow Glass/ITO/PTAA/Perovskite/C60/BCP/Cu	Willow Glass/ITO (RF-sputtering)	C60/BCP (thermal evaporation)	Blading-coating	PTAA (blade-coating)	Cu (evaporation)	42.9 (ap)	15.86	Dai <i>et al</i> [52]
2019	PET/PEDOT: PSS/CFE/PEDOT: PSS/Perovskite/PCBM/Ag	PEDOT:PSS/CFE/PET (slot-die coating via R2R)	PCBM (R2R slot-die coating)	R2R slot-die coating	PEDOT:PSS (R2R slot-die coating)	Ag (evaporation)	25 (ap)	10.9	Hu <i>et al</i> [219]
2020	Flexible-Substrate/ITO/F4-TCNQ:2T-NATA/Perovskite/C60/BCP/Ag	Flexible-Substrate/ITO (commercial)	C60/BCP (thermal evaporation)	Thermal evaporation	F4-TCNQ:2T-NATA (thermal evaporation)	Ag (evaporation)	16 (ac)	13.15	Lei <i>et al</i> [243]
2020	PET/ITO/PEDOT:EVA/perovskite/PCBM/BCP/Ag	PET/ITO (commercial)	PCBM/BCP (meniscus-coating)	Meniscus-coating	PEDOT:EVA	Ag (evaporation)	31.2	17.55	Meng <i>et al</i> [235]
2021	PET/ITO/PTAA/Perovskite/C60/BCP/Ag	PET/ITO (commercial)	C60/BCP (thermal evaporation)	N <sub>2</sub> assisted blade-coating	PTAA (blading-coating)	Ag (evaporation)	15.7 (ac)	10.5	Castriotta <i>et al</i> [244]
2021	PDMS/PEN/hc-PEDOT:PSS/PEDOT:PSS A14083:EVA/Perovskite/Di-g/PC61BM/BCP/Ag/PDMS	PDMS/PEN/hc-PEDOT:PSS (meniscus-coating)	PC61BM/BCP (meniscus-coating)	Meniscus-coating + vacuum oven annealing	PEDOT:PSS:EVA (meniscus-coating)	Ag (evaporation)	21.82 (ac)	15.01	Meng <i>et al</i> [169]
2021	PEN/hc-PEDOT:PSS/NiOx/Perovskite/PC61BM/BCP/Ag	PEN/hc-PEDOT:PSS (slot-die coating via R2R)	PC61BM/BCP (meniscus-coating)	Meniscus-coating	NiOx (meniscus-coating)	Ag (evaporation)	15 (ac)	16.15	Wang <i>et al</i> [241]
2021	PEN/hc-PEDOT:PSS/NiOx/Perovskite/PCBM/Ag	PEN/hc-PEDOT:PSS (meniscus-coating)	PCBM/BCP (meniscus-coating)	Meniscus-coating	NiOx (meniscus-coating)	Ag (evaporation)	25 (ac)	14.74	Yang <i>et al</i> [246]
2022	PEN/ITO/Bio-IL/Perovskite/PC61BM/BCP/Ag	PEN/ITO (commercial)	PC61BM/BCP (meniscus-coating)	Meniscus-coating	Bio-IL (meniscus-coating)	Ag (evaporation)	14.63 (ac)	16.87	Fan <i>et al</i> [247]

Abbreviations: (ap), aperture area; (ac), active area.

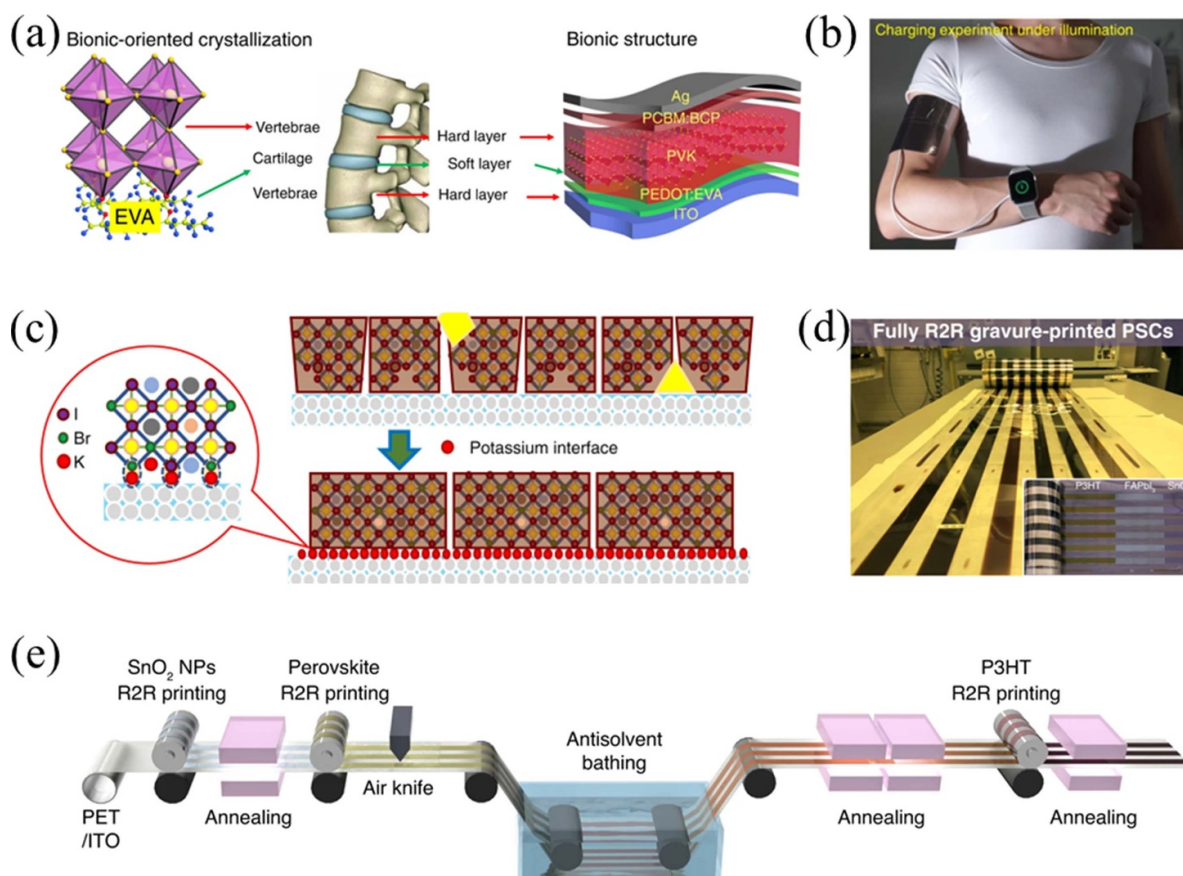


**Figure 11.** (a) Structure of F-PSC inspired by vertebrae, and (b) the application as wearable power sources. Reproduced from [235]. CC BY 4.0. (c) The schematics for potassium interfacial passivation. Reproduced from [238]. CC BY 4.0. (d) Photograph of fully R2R gravure-printed PSCs. (e) Schematics of R2R processing procedure for F-PSMs. Reproduced from [239]. CC BY 4.0.

## 7.5. Towards commercialization

Flexible perovskite solar cells (F-PSCs) have received tremendous attention owing to their huge advantages of flexibility, high power-per-weight, portability and low-cost roll-to-roll fabrication. Unfortunately, even though the certified efficiencies of single-junction flexible PSCs have reached 23.8% [13], large-area F-PSMs fabricated by scalable methods are quite limited. The present photoelectric functional materials (perovskite, interface and electrode materials), module configuration and fabrication technologies (spin-coating, slot-die printing and so on) are not matched with the industrial mass production of PSCs or PSMs. Even if the rational device configuration and deposition techniques are selected, the serious efficiency loss of large-scale structural design and manufacturing process are still the bottlenecks that limit the commercialization transition for the F-PSMs, which needs to be further investigated.

## 8. Perovskite indoor photovoltaics

Due to the increasing demand for self-powered electronic devices, indoor photovoltaics (IPVs) have gained significant attention and developed quickly. Bulky power supplies on everyday electronics become a burden, shortening the lifespan

of mobile devices. As a result, these stand-alone, low-power and off-grid electronic devices place new demands on the cost, size, weight and efficiency of wireless powered equipment [256]. IPVs can convert indoor light into electrical energy and become a powerful technology in IoT systems. In recent years, IPVs based on organic photovoltaics (OPVs), dye-sensitized (DSSCs), GaAs and amorphous silicon (a-Si) have developed rapidly [257–260]. However, these types of indoor photovoltaic devices have the limitations of high cost, mismatch of band gap under indoor light, difficulty in fabricating flexible devices, and relatively low efficiency. Therefore, it is critical to create a class of straightforward, affordable, and lightweight self-powered devices for IoTs [261]. The advantages of perovskite indoor photovoltaics (PIPVs), such as low cost, easily fabricated flexible devices, and flexibly adjustable band gaps, increase the prospect of indoor commercialization, which is more in line with the requirements of IoT systems [169, 253, 262, 263]. Cost, efficiency, and stability taken together with IPV's level determine if it can have a prominent place in the current competitive photovoltaic technology industry. [264].

### 8.1. Advantages of perovskites in IPVs

PIPVs require large-area flexible manufacturing techniques due to the characteristics of durability, wearability, and

portability of IoT systems. The continuous R2R procedure could produce perovskite thin films much more quickly and cheaply than alternative production techniques. Zuo *et al* showed how to fabricate devices using a 6.25 cm<sup>2</sup> flexible substrate and a blow-assisted pouring process with the assistance of NH<sub>4</sub>Cl additive using R2R in air, with a PCE above 11% [265]. Kim *et al* used gravure printing for the first time in 2019 to create flexible perovskite devices [266]. The perovskite layer was fabricated with a two-step sequential process with partial R2R treatment. The PCE of the matching device was 9.7%. The production cost can be effectively decreased by using R2R approach. However, the low PCE of this method limits its future development. In order to enhance the functionality of the devices, flexible large-area PIPV also necessitates the development of cutting-edge techniques. These include component engineering, interface engineering, and solvent atmosphere engineering.

Perovskite materials are particularly desirable in IPVVs by virtue of their wide tunable band gap. Perovskite crystals are commonly ABX<sub>3</sub> structures, where A-site is a monovalent cation (FA<sup>+</sup>, MA<sup>+</sup>, and Cs<sup>+</sup>), B-site is a divalent metal cation (Pb<sup>2+</sup> and Sn<sup>2+</sup>), and X-site is a halide anion (Cl<sup>-</sup>, Br<sup>-</sup> and I<sup>-</sup>) [267]. The initial PSCs started with methylammonium lead iodide (MAPbI<sub>3</sub>) with a band gap of 1.55 eV [268], which can be extended to other perovskite compositions by replacing different sites. Through compositional engineering with mixed different cations or anions, the band gap of perovskites can be continuously tuned from infrared (1.15 eV) to UV (3 eV), making them excellent candidates for IPVVs as well as for the creation of PVs in unique settings like microwave and infrared. The performance of PSCs serves as the foundation for the creation of highly effective PIPVs. When creating PIPVs, it is possible to prevent performance degradation brought on by technical difficulties by choosing bandgap-matched perovskite materials from advanced PSCs. High-performance PIPVs can currently be made using all-inorganic perovskite materials CsPbBrI<sub>2</sub> (1.89 eV) and CsPbI<sub>3</sub> (1.7 eV) to match the spectrum of indoor light sources (200–700 nm) [269]. It is undeniable that as photovoltaic technology advances, a wider range of perovskite materials can be employed to create high-performance PIPVs.

## 8.2. Accurate measurement of IPVVs

The performance of photovoltaic devices differs significantly between indoor and outdoor environments. Therefore, a precise assessment of IPVVs' photovoltaic performance is essential. A number of interior lighting options, such as indirect sunlight, incandescent, halogen, fluorescent, LED, and other low-intensity (200–1000 lux) light sources are used in our daily life. Using the matching incident power, the illuminance of an indoor light source can be expressed using the following formula [270]:

$$E_v = K_m \times \int_0^{\infty} E_{\lambda} \times V(\lambda) d\lambda \quad (6)$$

where  $V(\lambda)$  denotes the CIE spectral luminosity factor for human photopic vision and  $K_m$  equals to 683 lm W<sup>-1</sup>.

For accurate calibration of indoor light sources, Wong *et al* and colleagues recommended utilizing a general-purpose LED light meter with National Institute of Standards and Technology-traceable calibration. They also advise utilizing the maximum power point  $P_{\max}$  and PCE values to precisely evaluate device performance [270]. Cui *et al* suggested that the following elements be included in an accurate IPV test [271]. (1) The indoor photovoltaic measurement light source's instability should be kept below 2%. The test needs to be carried out in a well-lit location with a less than 2% spatial distribution in light intensity. (2) Use a mask that is the same size as or greater than the cell transparent substrate to test PCE. (3) Spectrometers rather than illuminometers are more suitable for calibrating interior light sources. (4) The test accuracy can be validated by comparing the  $J_{sc}$  (EQE) and actual  $J_{sc}$  differences by no more than 5%. Generally, choosing an appropriate light source and calibrating the light source using a spectrometer are essential steps. The performance of IPVVs should also be described in terms of light source parameters, like light intensity and lux, and power parameters.

## 8.3. Progresses and perspectives

In 2015, Chen *et al* firstly reported the low-light performance of perovskite photovoltaics and device engineering specifically for this application [272]. This work effectively reduced traps in perovskite active layer by improving the fabricating process of the electron-transporting layer. The optimized device exhibited a higher fill factor at a light intensity of 100 lux. Finally, they achieved a PCE of 22.5%–27.4% at 100–1000 lux for small-area devices, and 20.4% for large-area devices (5.44 cm<sup>2</sup>) under 600–1000 lux. This was strongly competitive with the expensive GaAs and AlGaAs photovoltaics reported at that time (19.4% and 21.1%) and the state-of-the-art DSSC, OPV submodules (14.1% and 14.3%) on the market. In 2018, Li *et al* used 1-butyl-3-methylimidazolium tetrafluoroborate ionic liquid for the first time as a modification layer for [6,6]-phenyl-C61-butyric acid methyl ester (PCBM) in an inverted PSCs for the first time [273]. The addition not only flattened the interfacial contact between the PCBM and the electrode, but also facilitated electron transport and extraction due to the surface passivation of the trap states. The resulting PSCs exhibited a record indoor PCE of 35.20% under a fluorescent lamp of 1000 lux. The breakthrough efficiency guided further research and development of PIPVs. Three years later, He *et al* achieved record low-light PIPVs efficiency over 40% with bulk trap passivation using micron-thick perovskite films in 2021 [274].

Considering the matching of perovskite bandgap and indoor light source spectrum (200–700 nm), all-inorganic perovskite materials CsPbBrI<sub>2</sub> (1.89 eV) can be used to fabricate high-performance PIPVs. Wang *et al* firstly used (NH<sub>4</sub>)<sub>2</sub>C<sub>2</sub>O<sub>4</sub>H<sub>2</sub>O to treat CsPbBrI<sub>2</sub> perovskite films during spin coating process, thereby improving the charge transfer ability and reducing ideality factors of perovskite [275]. Afterwards, they investigated the smelting multiple

recrystallization strategy and its effect on the morphology, composition and defects of CsPbBrI<sub>2</sub> films [276]. The crystal structure was optimized, yielding high-quality perovskite films with significantly reduced trap density of states. The final optimized photovoltaic device exhibited a higher indoor PCE of 33.50% (2956 K,  $P_{in}$ : 334.41  $\mu\text{W cm}^{-2}$ ) under LED light source. Compared with rigid devices, flexible PSCs can provide a more suitable surface for indoor small electronics, making them promising for indoor applications. Chen *et al* conducted research on indoor photovoltaics of flexible PSCs for the first time [277]. They utilized a 3D cross-linking agent called borax that could permeate grain boundaries of perovskite films to achieve all-round stress release. This strategy improved the phase and mechanical stability of perovskite films under large temperature changes and external forces. The merit of low trap density under indoor light enabled the device to exhibit an excellent indoor PCE of 31.85% at 1062 lux (LED, 2956 K). Additionally, because indoor photovoltaics are more possible to contact with humans, the toxicity of photovoltaic devices is also an important consideration for final market selection. Yang *et al* applied lead-free tin-based perovskites to IPV for the first time [278]. They introduced catechins into the perovskite layer to inhibit oxidation of Sn<sup>2+</sup>, resulting in FA<sub>0.75</sub>MA<sub>0.25</sub>SnI<sub>2</sub>Br films with lower Sn<sup>4+</sup> ratio. The final optimized device achieved a maximum PCE of 12.81% at 1000 lux. This work further advances the potential of lead-free PSCs for IPV applications.

## 9. Future perspectives

In this review, we have systematically analyzed the current status, remaining challenges and promising directions towards commercialization for perovskite solar cells. PSCs have made remarkable achievements during the past few years benefiting from the deeper understanding of the film formation process and increasingly mature fabrication techniques. Researches have been focused on the transition from lab to fab for both academia and industry. Currently, perovskite solar cells are in the early stages of industrialization, with a growing number of start-ups and new-energy enterprises starting to deploy production lines. With capital continuously pouring in, the industry community and academia need to hold a rational attitude at this moment and speed up the fundamental research to sweep away the hurdles in the way of commercialization.

One of the most critical factors influencing the commercialization of perovskite solar cells is the continuous advancement of up-scaling performance. Up to now, most reported PSMs still lag far behind in efficiency compared to small-area PSCs with a PCE over 26%. The PSMs with more than 20% efficiency are usually with an area of below 100 cm<sup>2</sup>. The highest record for large-scale perovskite solar modules was 19.9% with an active area of 810 cm<sup>2</sup>, which is less competitive compared with crystalline silicon module's 24.4% at 13 177 cm<sup>2</sup> [6]. There is still long way to go for the upscaling of PSCs. Although perovskite inks that are compositionally favorable for large-scale manufacturing process are widely explored, it

is still challenging to achieve reproducible and homogenous large-area perovskite films. Besides, another key issue is to obtain all device layers by fully scalable fabrication methods, and the processing techniques for large-scale production still needs to be investigated.

Operational stability is also an intractable problem for PSMs. Except for the vulnerability of perovskite materials in outdoor conditions (such as humidity, temperature and light), halide ions (such as I<sup>-</sup>) from the perovskite layer can rapidly erode metal electrodes by direct contact in the P2 scribe channels [279]. Thus, appropriate top electrodes need to be developed. Furthermore, it is necessary to explore effective external and internal encapsulation strategies to hinder degradation and lead leakage. Ion migration or diffusion should also be tackled. Moreover, it is significant to establish a standardized characterization protocol for suitable valuation of the results reported by different research groups from all over the world. Still, we believe that the continuous printing of high-performance PSMs can be achieved with the reasonable compositional engineering, the rational design of modular structure and the development of appropriate printing technology.

Apart from the researches targeting perovskite solar cells and modules, encapsulation, as a crucial step in industrialization, should not be neglected, owing to their powerful role in both enhancing stability and blocking lead leakage. In general, the encapsulation technology for perovskite devices has developed rapidly in recent years. It has enabled increasingly stable perovskite devices to approach commercial standards, which is a huge milestone. However, there are still some immature technical problems in the encapsulation technology of perovskite devices, including large-scale, mechanization and cost, etc. Methods to solve these problems include using mature CVD, ALD, and other technologies. Besides, encapsulation technology can also focus on other characteristics of perovskite devices such as flexibility, stretchability, heat dissipation, self-cleaning, and aesthetics, etc. As the last step of perovskite commercialization, the encapsulation technology needs to keep up with the development of perovskite devices and prepare for the commercialization of perovskite.



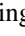
Although the current photovoltaic market is still dominated by crystalline Si solar cells, the space for cost reduction and efficiency improvement of Si solar cells is getting smaller and smaller. Given this, PSCs become promising alternatives with great upside potential. Although challenging, we believe that with continuous research and investment, PSCs have the potential to revolutionize the solar energy industry, and offer a promising pathway towards a sustainable and low-carbon future.

## Acknowledgments

We thank the National Key Research and Development Program of China (2022YFB3803300 and 2023YFE0116800), and Beijing Natural Science Foundation (IS23037).



## ORCID iDs

Yan Jiang  <https://orcid.org/0000-0001-7665-1174>  
 Liang Li  <https://orcid.org/0000-0003-0708-7762>  
 Liming Ding  <https://orcid.org/0000-0001-6437-9150>

## References

- [1] National Renewable Energy Laboratory Best research-cell efficiencies (available at: [www.nrel.gov/pv/cell-efficiency.html](http://www.nrel.gov/pv/cell-efficiency.html)) (Accessed 8 2023)
- [2] Jeong M *et al* 2020 Stable perovskite solar cells with efficiency exceeding 24.8% and 0.3-V voltage loss *Science* **369** 1615
- [3] Jeong J *et al* 2021 Pseudo-halide anion engineering for  $\alpha$ -FAPbI<sub>3</sub> perovskite solar cells *Nature* **592** 381–5
- [4] Min H *et al* 2021 Perovskite solar cells with atomically coherent interlayers on SnO<sub>2</sub> electrodes *Nature* **598** 444–50
- [5] Solarbe Photovoltaics New record achieved by Shenzhen Infinite Solar Technology Co., Ltd (available at: <https://news.solarbe.com/202302/14/364938.html>) (Accessed 4 2023)
- [6] National Renewable Energy Laboratory Champion module efficiencies (available at: [www.nrel.gov/pv/module-efficiency.html](http://www.nrel.gov/pv/module-efficiency.html)) (Accessed 8 2022)
- [7] Mei A *et al* 2020 Stabilizing perovskite solar cells to IEC61215:2016 standards with over 9,000-h operational tracking *Joule* **4** 2646–60
- [8] Shi L *et al* 2020 Gas chromatography–mass spectrometry analyses of encapsulated stable perovskite solar cells *Science* **368** eaba2412
- [9] Grancini G *et al* 2017 One-Year stable perovskite solar cells by 2D/3D interface engineering *Nat. Commun.* **8** 15684
- [10] Li H and Zhang W 2020 Perovskite tandem solar cells: from fundamentals to commercial deployment *Chem. Rev.* **120** 9835–950
- [11] Ho-Baillie A W Y, Zheng J, Mahmud M A, Ma F-J, McKenzie D R and Green M A 2021 Recent progress and future prospects of perovskite tandem solar cells *Appl. Phys. Rev.* **8** 041307
- [12] Aydin E, Allen T G, De Bastiani M, Razzaq A, Xu L, Ugur E, Liu J and De Wolf S 2024 Pathways toward commercial perovskite/silicon tandem photovoltaics *Science* **383** eadh3849
- [13] Chen Z *et al* 2023 Perovskite grain-boundary manipulation using room-temperature dynamic self-healing “ligaments” for developing highly stable flexible perovskite solar cells with 23.8% efficiency *Adv. Mater.* **35** 2300513
- [14] Xia J *et al* 2022 Tailoring electric dipole of hole-transporting material p-dopants for perovskite solar cells *Joule* **6** 1689–709
- [15] Zhu X, Yang D, Yang R, Yang B, Yang Z, Ren X, Zhang J, Niu J, Feng J and Liu S F 2017 Superior stability for perovskite solar cells with 20% efficiency using vacuum co-evaporation *Nanoscale* **9** 12316–23
- [16] Li P, Liang C, Bao B, Li Y, Hu X, Wang Y, Zhang Y, Li F, Shao G and Song Y 2018 Inkjet manipulated homogeneous large size perovskite grains for efficient and large-area perovskite solar cells *Nano Energy* **46** 203–11
- [17] Abdollahi Nejand B *et al* 2022 Scalable two-terminal all-perovskite tandem solar modules with a 19.1% efficiency *Nat. Energy* **7** 620–30
- [18] Green M A, Dunlop E D, Siefer G, Yoshita M, Kopidakis N, Bothe K and Hao X 2023 Solar cell efficiency tables (version 61) *Prog. Photovolt. Res. Appl.* **31** 3–16
- [19] Microquanta Company News center (available at: [www.microquanta.com/](http://www.microquanta.com/)) (Accessed 2 2024)
- [20] GCL Company News center (available at: [www.gcl-perovskite.com/wm/](http://www.gcl-perovskite.com/wm/)) (Accessed 2 2024)
- [21] Oxford PV Company News center (available at: [www.oxfordpv.com/](http://www.oxfordpv.com/)) (Accessed 2 2024)
- [22] Wondersolar Company News center (available at: <http://wondersolar.cn/en/nd.jsp?id=11>) (Accessed 2 2024)
- [23] Utmolight Company News center (available at: [www.utmolight.com/](http://www.utmolight.com/)) (Accessed 2 2024)
- [24] IEA Renewable energy market update (available at: [https://iea.blob.core.windows.net/assets/67ff3040-dc78-4255-a3d4-b1e5b2be41c8/RenewableEnergyMarketUpdate\\_June2023.pdf](https://iea.blob.core.windows.net/assets/67ff3040-dc78-4255-a3d4-b1e5b2be41c8/RenewableEnergyMarketUpdate_June2023.pdf)) (Accessed 2 2024)
- [25] Gong J, Darling S B and You F 2015 Perovskite photovoltaics: life-cycle assessment of energy and environmental impacts *Energy Environ. Sci.* **8** 1953–68
- [26] Chang N L, Yi Ho-Baillie A W, Basore P A, Young T L, Evans R and Egan R J 2017 A manufacturing cost estimation method with uncertainty analysis and its application to perovskite on glass photovoltaic modules *Prog. Photovolt. Res. Appl.* **25** 390–405
- [27] Ding Y *et al* 2022 Single-crystalline TiO<sub>2</sub> nanoparticles for stable and efficient perovskite modules *Nat. Nanotechnol.* **17** 598–605
- [28] Turkevych I *et al* 2019 Strategic advantages of reactive polyiodide melts for scalable perovskite photovoltaics *Nat. Nanotechnol.* **14** 57–63
- [29] Yoo J W, Jang J, Kim U, Lee Y, Ji S-G, Noh E, Hong S, Choi M and Seok S I 2021 Efficient perovskite solar mini-modules fabricated via bar-coating using 2-methoxyethanol-based formamidinium lead tri-iodide precursor solution *Joule* **5** 2420–36
- [30] Bu T *et al* 2022 Modulating crystal growth of formamidinium–caesium perovskites for over 200 cm<sup>2</sup> photovoltaic sub-modules *Nat. Energy* **7** 528–36
- [31] Vesce L, Stefanelli M, Rossi F, Castriotta L A, Basosi R, Parisi M L, Sinicropi A and Di Carlo A 2024 Perovskite solar cell technology scaling-up: eco-efficient and industrially compatible sub-module manufacturing by fully ambient air slot-die/blade meniscus coating *Prog. Photovolt. Res. Appl.* **32** 115–29
- [32] Abzieher T *et al* 2019 Electron-beam-evaporated nickel oxide hole transport layers for perovskite-based photovoltaics *Adv. Energy Mater.* **9** 1802995
- [33] Zhao X, Wang Z, Li W, Sun S, Xu H, Zhou P, Xu J, Lin Y and Liu Y 2020 Photoassisted electroforming method for reliable low-power organic–inorganic perovskite memristors *Adv. Funct. Mater.* **30** 1910151
- [34] Rolston N, Scheideler W J, Flick A C, Chen J P, Elmaraghi H, Sleugh A, Zhao O, Woodhouse M and Dauskardt R H 2020 Rapid open-air fabrication of perovskite solar modules *Joule* **4** 2675–92
- [35] Yang F, Jang D, Dong L, Qiu S, Distler A, Li N, Brabec C J and Egelhaaf H J 2021 Upscaling solution-processed perovskite photovoltaics *Adv. Energy Mater.* **11** 2101973
- [36] Bu T *et al* 2021 Lead halide-templated crystallization of methylamine-free perovskite for efficient photovoltaic modules *Science* **372** 1327–32
- [37] Park N-G and Zhu K 2020 Scalable fabrication and coating methods for perovskite solar cells and solar modules *Nat. Rev. Mater.* **5** 333–50
- [38] Wang Y *et al* 2021 Cation-size mismatch and interface stabilization for efficient NiO<sub>x</sub>-based inverted perovskite solar cells with 21.9% efficiency *Nano Energy* **88** 106285
- [39] Yang Z *et al* 2021 Slot-die coating large-area formamidinium-cesium perovskite film for efficient and stable parallel solar module *Sci. Adv.* **7** eabg3749

- [40] Dai X, Chen S, Deng Y, Wood A, Yang G, Fei C and Huang J 2022 Pathways to high efficiency perovskite monolithic solar modules *PRX Energy* **1** 013004
- [41] Wang Y, Arumugam G M, Mahmoudi T, Mai Y and Hahn Y-B 2021 A critical review of materials innovation and interface stabilization for efficient and stable perovskite photovoltaics *Nano Energy* **87** 106141
- [42] Moon S-J, Yum J-H, Lofgren L, Walter A, Sansonnens L, Benkhaira M, Nicolay S, Bailat J and Ballif C 2015 Laser-scribing patterning for the production of organometallic halide perovskite solar modules *IEEE J. Photovolt.* **5** 1087–92
- [43] Palma A L, Matteocci F, Agresti A, Pescetelli S, Calabro E, Vesce L, Christiansen S, Schmidt M and Di Carlo A 2017 Laser-patterning engineering for perovskite solar modules with 95% aperture ratio *IEEE J. Photovolt.* **7** 1674–80
- [44] Wilkinson B, Chang N L, Green M A and Ho-Baillie A W Y 2018 Scaling limits to large area perovskite solar cell efficiency *Prog. Photovolt. Res. Appl.* **26** 659–74
- [45] Extance A 2019 The reality behind solar power's next star material *Nature* **570** 429–32
- [46] Ren A *et al* 2020 Efficient perovskite solar modules with minimized nonradiative recombination and local carrier transport losses *Joule* **4** 1263–77
- [47] Li Z, Klein T R, Kim D H, Yang M, Berry J J, van Hest M F A M and Zhu K 2018 Scalable fabrication of perovskite solar cells *Nat. Rev. Mater.* **3** 18017
- [48] Eldada L A, Heben M J, Song Z, Watthage S C, Phillips A B, Liyanage G K, Khanal R R, Tompkins B L, Ellingson R J and Heben M J 2015 Investigation of degradation mechanisms of perovskite-based photovoltaic devices using laser beam induced current mapping *Proc. SPIE* **9561** 956107
- [49] Chen S, Dai X, Xu S, Jiao H, Zhao L and Huang J 2021 Stabilizing perovskite-substrate interfaces for high-performance perovskite modules *Science* **373** 902–7
- [50] Wu W Q *et al* 2019 Bilateral alkylamine for suppressing charge recombination and improving stability in blade-coated perovskite solar cells *Sci. Adv.* **5** eaav8925
- [51] Deng Y, Xu S, Chen S, Xiao X, Zhao J and Huang J 2021 Defect compensation in formamidinium–caesium perovskites for highly efficient solar mini-modules with improved photostability *Nat. Energy* **6** 633–41
- [52] Dai X, Deng Y, Van Brackle C H, Chen S, Rudd P N, Xiao X, Lin Y, Chen B and Huang J 2019 Scalable fabrication of efficient perovskite solar modules on flexible glass substrates *Adv. Energy Mater.* **10** 1903108
- [53] Holzhey P and Saliba M 2018 A full overview of international standards assessing the long-term stability of perovskite solar cells *J. Mater. Chem. A* **6** 21794–808
- [54] Azmi R *et al* 2022 Damp heat-stable perovskite solar cells with tailored-dimensionality 2D/3D heterojunctions *Science* **376** 73–77
- [55] Li Z, Li B, Wu X, Sheppard S A, Zhang S, Gao D, Long N J and Zhu Z 2022 Organometallic-functionalized interfaces for highly efficient inverted perovskite solar cells *Science* **376** 416–20
- [56] Tsai H *et al* 2018 Light-induced lattice expansion leads to high-efficiency perovskite solar cells *Science* **360** 67–70
- [57] Li Z, Yang M J, Park J S, Wei S H, Berry J J and Zhu K 2016 Stabilizing perovskite structures by tuning tolerance factor: formation of formamidinium and cesium lead iodide solid-state alloys *Chem. Mater.* **28** 284–92
- [58] Song Z N, Li C W, Chen C, McNatt J, Yoon W, Scheiman D, Jenkins P P, Ellingson R J, Heben M J and Yan Y F 2020 High remaining factors in the photovoltaic performance of perovskite solar cells after high-fluence electron beam irradiations *J. Phys. Chem. C* **124** 1330–6
- [59] Bella F, Griffini G, Correa-Baena J P, Saracco G, Gratzel M, Hagfeldt A, Turri S and Gerbaldi C 2016 Improving efficiency and stability of perovskite solar cells with photocurable fluoropolymers *Science* **354** 203–6
- [60] Zhao C, Chen B, Qiao X, Luan L, Lu K and Hu B 2015 Revealing underlying processes involved in light soaking effects and hysteresis phenomena in perovskite solar cells *Adv. Energy Mater.* **5** 1500279
- [61] Shao S *et al* 2016 Elimination of the light soaking effect and performance enhancement in perovskite solar cells using a fullerene derivative *Energy Environ. Sci.* **9** 2444–52
- [62] Meggiolaro D, Mosconi E and De Angelis F 2019 Formation of surface defects dominates ion migration in lead-halide perovskites *ACS Energy Lett.* **4** 779–85
- [63] Zhao Y *et al* 2020 Strain-activated light-induced halide segregation in mixed-halide perovskite solids *Nat. Commun.* **11** 6328
- [64] Mao W, Hall C R, Bernardi S, Cheng Y B, Widmer-Cooper A, Smith T A and Bach U 2021 Light-induced reversal of ion segregation in mixed-halide perovskites *Nat. Mater.* **20** 55–61
- [65] Kim H S, Seo J Y and Park N G 2016 Material and device stability in perovskite solar cells *ChemSusChem* **9** 2528–40
- [66] Supasai T, Rujisamphan N, Ullrich K, Chemseddine A and Ditttrich T 2013 Formation of a passivating  $\text{CH}_3\text{NH}_3\text{PbI}_3/\text{PbI}_2$  interface during moderate heating of  $\text{CH}_3\text{NH}_3\text{PbI}_3$  layers *Appl. Phys. Lett.* **103** 183906
- [67] Conings B *et al* 2015 Intrinsic thermal instability of methylammonium lead trihalide perovskite *Adv. Energy Mater.* **5** 1500477
- [68] Stoumpos C C, Malliakas C D and Kanatzidis M G 2013 Semiconducting tin and lead iodide perovskites with organic cations: phase transitions, high mobilities, and near-infrared photoluminescent properties *Inorg. Chem.* **52** 9019
- [69] Protesescu L, Yakunin S, Bodnarchuk M I, Krieg F, Caputo R, Hendon C H, Yang R X, Walsh A and Kovalenko M V 2015 Nanocrystals of cesium lead halide perovskites ( $\text{CsPbX}_3$ , X = Cl, Br, and I): novel optoelectronic materials showing bright emission with wide color gamut *Nano Lett.* **15** 3692–6
- [70] Bi E, Chen H, Xie F, Wu Y, Chen W, Su Y, Islam A, Gratzel M, Yang X and Han L 2017 Diffusion engineering of ions and charge carriers for stable efficient perovskite solar cells *Nat. Commun.* **8** 15330
- [71] Liu L *et al* 2018 Grain-boundary “patches” by in situ conversion to enhance perovskite solar cells stability *Adv. Mater.* **30** e1800544
- [72] Li Z *et al* 2017 Extrinsic ion migration in perovskite solar cells *Energy Environ. Sci.* **10** 1234–42
- [73] Yue Y *et al* 2016 Enhanced stability of perovskite solar cells through corrosion-free pyridine derivatives in hole-transporting materials *Adv. Mater.* **28** 10738–43
- [74] Aristidou N, Sanchez-Molina I, Chotchuangchutchaval T, Brown M, Martinez L, Rath T and Haque S A 2015 The role of oxygen in the degradation of methylammonium lead trihalide perovskite photoactive layers *Angew. Chem., Int. Ed. Engl.* **54** 8208–12
- [75] Kaltenbrunner M *et al* 2015 Flexible high power-per-weight perovskite solar cells with chromium oxide-metal contacts for improved stability in air *Nat. Mater.* **14** 1032–9
- [76] Jiang Y and Qi Y 2021 Metal halide perovskite-based flexible tandem solar cells: next-generation flexible photovoltaic technology *Mater. Chem. Front.* **5** 4833–50
- [77] Yang J, Bao Q, Shen L and Ding L 2020 Potential applications for perovskite solar cells in space *Nano Energy* **76** 105019

- [78] Tu Y, Wu J, Xu G, Yang X, Cai R, Gong Q, Zhu R and Huang W 2021 Perovskite solar cells for space applications: progress and challenges *Adv. Mater.* **33** e2006545
- [79] Jiang Y, Yang S-C, Jeangros Q, Pisoni S, Moser T, Buecheler S, Tiwari A N and Fu F 2020 Mitigation of vacuum and illumination-induced degradation in perovskite solar cells by structure engineering *Joule* **4** 1087–103
- [80] Cheacharoen R, Rolston N, Harwood D, Bush K A, Dauskardt R H and McGehee M D 2018 Design and understanding of encapsulated perovskite solar cells to withstand temperature cycling *Energy Environ. Sci.* **11** 144–50
- [81] Liu B, Zhang L, Jiang Y and Ding L 2022 Failure pathways of perovskite solar cells in space *J. Semicond.* **43** 100201–1
- [82] Kirmani A R *et al* 2022 Countdown to perovskite space launch: guidelines to performing relevant radiation-hardness experiments *Joule* **6** 1015–31
- [83] Miyazawa Y, Ikegami M, Chen H W, Ohshima T, Imaizumi M, Hirose K and Miyasaka T 2018 Tolerance of perovskite solar cell to high-energy particle irradiations in space environment *iScience* **2** 148–55
- [84] Chen S *et al* 2018 Atomic scale insights into structure instability and decomposition pathway of methylammonium lead iodide perovskite *Nat. Commun.* **9** 4807
- [85] Xiao C *et al* 2015 Mechanisms of electron-beam-induced damage in perovskite thin films revealed by cathodoluminescence spectroscopy *J. Phys. Chem. C* **119** 26904–11
- [86] Lang F, Joß M, Bundesmann J, Denker A, Albrecht S, Landi G, Neitzert H-C, Rappich J and Nickel N H 2019 Efficient minority carrier detrapping mediating the radiation hardness of triple-cation perovskite solar cells under proton irradiation *Energy Environ. Sci.* **12** 1634–47
- [87] Lang F *et al* 2020 Proton radiation hardness of perovskite tandem photovoltaics *Joule* **4** 1054–69
- [88] Lang F *et al* 2021 Proton-radiation tolerant all-perovskite multijunction solar cells *Adv. Energy Mater.* **11** 2102246
- [89] De Rossi F *et al* 2022 Neutron irradiated perovskite films and solar cells on PET substrates *Nano Energy* **93** 106879
- [90] Svanstrom S, Garcia Fernandez A, Sloboda T, Jacobsson T J, Rensmo H and Cappel U B 2021 X-ray stability and degradation mechanism of lead halide perovskites and lead halides *Phys. Chem. Chem. Phys.* **23** 12479–89
- [91] Boldyreva A G, Frolova L A, Zhidkov I S, Gutsev L G, Kurmaev E Z, Ramachandran B R, Petrov V G, Stevenson K J, Aldoshin S M and Troshin P A 2020 Unravelling the material composition effects on the gamma ray stability of lead halide perovskite solar cells: mAPbI<sub>3</sub> breaks the records *J. Phys. Chem. Lett.* **11** 2630–6
- [92] Boldyreva A G, Akbulatov A F, Tsarev S A, Luchkin S Y, Zhidkov I S, Kurmaev E Z, Stevenson K J, Petrov V G and Troshin P A 2019 gamma-ray-induced degradation in the triple-cation perovskite solar cells *J. Phys. Chem. Lett.* **10** 813–8
- [93] Yang S, Xu Z, Xue S, Kandlakunta P, Cao L and Huang J 2019 Organohalide lead perovskites: more stable than glass under gamma-ray radiation *Adv. Mater.* **31** e1805547
- [94] Berhe T A, Su W-N, Chen C-H, Pan C-J, Cheng J-H, Chen H-M, Tsai M-C, Chen L-Y, Dubale A A and Hwang B-J 2016 Organometal halide perovskite solar cells: degradation and stability *Energy Environ. Sci.* **9** 323–56
- [95] Bush K A *et al* 2017 23.6%-efficient monolithic perovskite/silicon tandem solar cells with improved stability *Nat. Energy* **2** 17009
- [96] Doherty T A S *et al* 2021 Stabilized tilted-octahedra halide perovskites inhibit local formation of performance-limiting phases *Science* **374** 1598–605
- [97] Yi C, Luo J, Meloni S, Boziki A, Ashari-Astani N, Grätzel C, Zakeeruddin S M, Röthlisberger U and Grätzel M 2016 Entropic stabilization of mixed A-cation ABX<sub>3</sub> metal halide perovskites for high performance perovskite solar cells *Energy Environ. Sci.* **9** 656–62
- [98] Saliba M *et al* 2016 Incorporation of rubidium cations into perovskite solar cells improves photovoltaic performance *Science* **354** 206–9
- [99] Xie F, Chen C-C, Wu Y, Li X, Cai M, Liu X, Yang X and Han L 2017 Vertical recrystallization for highly efficient and stable formamidinium-based inverted-structure perovskite solar cells *Energy Environ. Sci.* **10** 1942–9
- [100] Mu C, Pan J, Feng S, Li Q and Xu D 2017 Quantitative doping of chlorine in formamidinium lead trihalide (FAPbI<sub>3-x</sub>Cl<sub>x</sub>) for planar heterojunction perovskite solar cells *Adv. Energy Mater.* **7** 1601297
- [101] Zhao Y *et al* 2022 A bilayer conducting polymer structure for planar perovskite solar cells with over 1,400 hours operational stability at elevated temperatures *Nat. Energy* **7** 144–52
- [102] Chen Y *et al* 2019 Impacts of alkaline on the defects property and crystallization kinetics in perovskite solar cells *Nat. Commun.* **10** 1112
- [103] Wu Y, Yang X, Chen W, Yue Y, Cai M, Xie F, Bi E, Islam A and Han L 2016 Perovskite solar cells with 18.21% efficiency and area over 1 cm<sup>2</sup> fabricated by heterojunction engineering *Nat. Energy* **1** 16148
- [104] Kim M *et al* 2019 Methylammonium chloride induces intermediate phase stabilization for efficient perovskite solar cells *Joule* **3** 2179–92
- [105] Chen Q *et al* 2015 The optoelectronic role of chlorine in CH<sub>3</sub>NH<sub>3</sub>PbI<sub>3</sub>(Cl)-based perovskite solar cells *Nat. Commun.* **6** 7269
- [106] Lai H, Kan B, Liu T, Zheng N, Xie Z, Zhou T, Wan X, Zhang X, Liu Y and Chen Y 2018 Two-dimensional Ruddlesden-Popper perovskite with nanorod-like morphology for solar cells with efficiency exceeding 15 *J. Am. Chem. Soc.* **140** 11639–46
- [107] Dastidar S, Hawley C J, Dillon A D, Gutierrez-Perez A D, Spanier J E and Fafarman A T 2017 Quantitative phase-change thermodynamics and metastability of perovskite-phase cesium lead iodide *J. Phys. Chem. Lett.* **8** 1278–82
- [108] Han Q *et al* 2016 Single crystal formamidinium lead iodide (FAPbI<sub>3</sub>): insight into the structural, optical, and electrical properties *Adv. Mater.* **28** 2253–8
- [109] Min H, Kim M, Lee S U, Kim H, Kim G, Choi K, Lee J H and Seok S I 2019 Efficient, stable solar cells by using inherent bandgap of alpha-phase formamidinium lead iodide *Science* **366** 749–53
- [110] Wang Q, Chen B, Liu Y, Deng Y, Bai Y, Dong Q and Huang J 2017 Scaling behavior of moisture-induced grain degradation in polycrystalline hybrid perovskite thin films *Energy Environ. Sci.* **10** 516–22
- [111] Yin W J, Shi T and Yan Y 2014 Unique properties of halide perovskites as possible origins of the superior solar cell performance *Adv. Mater.* **26** 4653–8
- [112] Long R, Liu J and Prezhdo O V 2016 Unravelling the effects of grain boundary and chemical doping on electron-hole recombination in CH<sub>3</sub>NH<sub>3</sub>PbI<sub>3</sub> perovskite by time-domain atomistic simulation *J. Am. Chem. Soc.* **138** 3884–90
- [113] Li X, Zhang W, Wang Y-C, Zhang W, Wang H-Q and Fang J 2018 In-situ cross-linking strategy for efficient and operationally stable methylammonium lead iodide solar cells *Nat. Commun.* **9** 3806



- [114] Fan Z *et al* 2017 Layer-by-layer degradation of methylammonium lead tri-iodide perovskite microplates *Joule* **1** 548–62
- [115] Aristidou N, Eames C, Sanchez-Molina I, Bu X, Kosco J, Islam M S and Haque S A 2017 Fast oxygen diffusion and iodide defects mediate oxygen-induced degradation of perovskite solar cells *Nat. Commun.* **8** 15218
- [116] Wang R *et al* 2019 Constructive molecular configurations for surface-defect passivation of perovskite photovoltaics *Science* **366** 1509–13
- [117] Zheng X, Chen B, Dai J, Fang Y, Bai Y, Lin Y, Wei H, Zeng X C and Huang J 2017 Defect passivation in hybrid perovskite solar cells using quaternary ammonium halide anions and cations *Nat. Energy* **2** 17102
- [118] Suo J *et al* 2024 Multifunctional sulfonium-based treatment for perovskite solar cells with less than 1% efficiency loss over 4,500-h operational stability tests *Nat. Energy* **9** 172–83
- [119] Yang S *et al* 2019 Stabilizing halide perovskite surfaces for solar cell operation with wide-bandgap lead oxysalts *Science* **365** 473–8
- [120] Wang Y, Wu T, Barbaud J, Kong W, Cui D, Chen H, Yang X and Han L 2019 Stabilizing heterostructures of soft perovskite semiconductors *Science* **365** 687–91
- [121] Li X, Zhang W, Guo X, Lu C, Wei J and Fang J 2022 Constructing heterojunctions by surface sulfidation for efficient inverted perovskite solar cells *Science* **375** 434–7
- [122] Zhang H *et al* 2018 Improving the stability and performance of perovskite solar cells via off-the-shelf post-device ligand treatment *Energy Environ. Sci.* **11** 2253–62
- [123] Liu Y *et al* 2019 Ultrahydrophobic 3D/2D fluoroarene bilayer-based water-resistant perovskite solar cells with efficiencies exceeding 22 *Sci. Adv.* **5** eaaw2543
- [124] You J *et al* 2016 Improved air stability of perovskite solar cells via solution-processed metal oxide transport layers *Nat. Nanotechnol.* **11** 75–81
- [125] Chen W *et al* 2015 Efficient and stable large-area perovskite solar cells with inorganic charge extraction layers *Science* **350** 944–8
- [126] Wu S *et al* 2019 A chemically inert bismuth interlayer enhances long-term stability of inverted perovskite solar cells *Nat. Commun.* **10** 1161
- [127] Li X, Fu S, Liu S, Wu Y, Zhang W, Song W and Fang J 2019 Suppressing the ions-induced degradation for operationally stable perovskite solar cells *Nano Energy* **64** 103962
- [128] Abate A *et al* 2015 Silolothiophene-linked triphenylamines as stable hole transporting materials for high efficiency perovskite solar cells *Energy Environ. Sci.* **8** 2946–53
- [129] Wang Y *et al* 2019 Dopant-free small-molecule hole-transporting material for inverted perovskite solar cells with efficiency exceeding 21% *Adv. Mater.* **31** e1902781
- [130] Ren M, Wang J, Xie X, Zhang J and Wang P 2019 Double-helicene-based hole-transporter for perovskite solar cells with 22% efficiency and operation durability *ACS Energy Lett.* **4** 2683–8
- [131] Wang J, Wang Y, Xie X, Ren Y, Zhang B, He L, Zhang J, Wang L-D and Wang P 2021 A helicene-based molecular semiconductor enables 85 °C stable perovskite solar cells *ACS Energy Lett.* **6** 1764–72
- [132] Christians J A, Fung R C and Kamat P V 2014 An inorganic hole conductor for organo-lead halide perovskite solar cells. Improved hole conductivity with copper iodide *J. Am. Chem. Soc.* **136** 758–64
- [133] Qin P, Tanaka S, Ito S, Tetreault N, Manabe K, Nishino H, Nazeeruddin M K and Gratzel M 2014 Inorganic hole conductor-based lead halide perovskite solar cells with 12.4% conversion efficiency *Nat. Commun.* **5** 3834
- [134] Tan B *et al* 2019 LiTFSI-free spiro-OMeTAD-based perovskite solar cells with power conversion efficiencies exceeding 19% *Adv. Energy Mater.* **9** 1901519
- [135] Li X, Fu S, Zhang W, Ke S, Song W and Fang J 2020 Chemical anti-corrosion strategy for stable inverted perovskite solar cells *Sci. Adv.* **6** eabd1580
- [136] Guarnera S, Abate A, Zhang W, Foster J M, Richardson G, Petrozza A and Snaith H J 2015 Improving the long-term stability of perovskite solar cells with a porous Al<sub>2</sub>O<sub>3</sub> buffer layer *J. Phys. Chem. Lett.* **6** 432–7
- [137] Domanski K, Correa-Baena J P, Mine N, Nazeeruddin M K, Abate A, Saliba M, Tress W, Hagfeldt A and Gratzel M 2016 Not all that glitters is gold: metal-migration-induced degradation in perovskite solar cells *ACS Nano* **10** 6306–14
- [138] Wu W Q *et al* 2018 Molecular doping enabled scalable blading of efficient hole-transport-layer-free perovskite solar cells *Nat. Commun.* **9** 1625
- [139] Mei A *et al* 2014 A hole-conductor-free, fully printable mesoscopic perovskite solar cell with high stability *Science* **345** 295–8
- [140] Que M, Zhang B, Chen J, Yin X and Yun S 2021 Carbon-based electrodes for perovskite solar cells *Mater. Adv.* **2** 5560–79
- [141] Ku Z, Rong Y, Xu M, Liu T and Han H 2013 Full printable processed mesoscopic CH<sub>3</sub>NH<sub>3</sub>PbI<sub>3</sub>/TiO<sub>2</sub> heterojunction solar cells with carbon counter electrode *Sci. Rep.* **3** 3132
- [142] Aung S K K, Vijayan A, Karimipour M, Seetawan T and Boschloo G 2023 Reduced hysteresis and enhanced air stability of low-temperature processed carbon-based perovskite solar cells by surface modification *Electrochim. Acta* **443** 141935
- [143] Deng F, Sun X, Lv X, Li Y, Li S, Zheng Y-Z and Tao X 2021 All room-temperature processing efficient planar carbon-based perovskite solar cells *J. Power Sources* **489** 229345
- [144] Bogachuk D *et al* 2020 Low-temperature carbon-based electrodes in perovskite solar cells *Energy Environ. Sci.* **13** 3880–916
- [145] Liu J *et al* 2024 Electron injection and defect passivation for high-efficiency mesoporous perovskite solar cells *Science* **383** 1198–204
- [146] Stefanelli M, Vesce L and Di Carlo A 2023 Upscaling of carbon-based perovskite solar module *Nanomaterials* **13** 313
- [147] Xu M *et al* 2020 Efficient triple-mesoscopic perovskite solar mini-modules fabricated with slot-die coating *Nano Energy* **74** 104842
- [148] World Health Organization Lead poisoning (available at: [www.who.int/news-room/fact-sheets/detail/lead-poisoning-and-health](http://www.who.int/news-room/fact-sheets/detail/lead-poisoning-and-health)) (Accessed 8 2022)
- [149] Babayigit A, Ethirajan A, Muller M and Conings B 2016 Toxicity of organometal halide perovskite solar cells *Nat. Mater.* **15** 247–51
- [150] Florence T M, Lilley S G and Stauber J L 1988 Skin absorption of lead *Lancet* **332** 157–8
- [151] United Nations Environment Programme 1977 Lead—environmental health criteria 3 (available at: <http://hdl.handle.net/20.500.11822/29263>) (Accessed 8 2022)
- [152] Benmessaoud I R, Mahul-Mellier A-L, Horváth E, Maco B, Spina M, Lashuel H A and Forró L 2016 Health hazards of methylammonium lead iodide based perovskites: cytotoxicity studies *Toxicol. Res.* **5** 407–19
- [153] Kwak J I, Kim L and An Y J 2021 Sublethal toxicity of PbI<sub>2</sub> in perovskite solar cells to fish embryos (Danio rerio and Oryzias latipes): deformity and growth inhibition *Sci. Total Environ.* **771** 145388

- [154] Li J, Cao H-L, Jiao W-B, Wang Q, Wei M, Cantone I, Lü J and Abate A 2020 Biological impact of lead from halide perovskites reveals the risk of introducing a safe threshold *Nat. Commun.* **11** 1–5
- [155] Ravi V K, Mondal B, Nawale V V and Nag A 2020 Don't let the lead out: new material chemistry approaches for sustainable lead halide perovskite solar cells *ACS Omega* **5** 29631–41
- [156] Ministry of Ecology and Environment of the People's Republic of China Integrated wastewater discharge standard (available at: [www.mee.gov.cn/ywgz/fgbz/bz/bzwb/shjbh/swrwpfbz/199801/t19980101\\_66568.shtml](http://www.mee.gov.cn/ywgz/fgbz/bz/bzwb/shjbh/swrwpfbz/199801/t19980101_66568.shtml)) (Accessed 8 2022)
- [157] The standardization administration of China Standards for drinking water quality (available at: <http://openstd.samr.gov.cn/bzgk/gb/newGbInfo?hcno=73D81F4F3615DDB2C5B1DD6BFC9DEC86>) (Accessed 8 2022)
- [158] U.S. Environmental Protection Agency 2022 Drinking water requirements for states and public water systems (available at: [www.epa.gov/dwreginfo/lead-and-copper-rule](http://www.epa.gov/dwreginfo/lead-and-copper-rule))
- [159] Wu P, Wang S, Li X and Zhang F 2022 Beyond efficiency fever: preventing lead leakage for perovskite solar cells *Matter* **5** 1137–61
- [160] Luo H, Li P, Ma J, Han L, Zhang Y and Song Y 2022 Sustainable Pb management in perovskite solar cells toward eco-friendly development *Adv. Energy Mater.* **12** 2201242
- [161] Jiang Y, Qiu L, Juarez-Perez E J, Ono L K, Hu Z, Liu Z, Wu Z, Meng L, Wang Q and Qi Y 2019 Reduction of lead leakage from damaged lead halide perovskite solar modules using self-healing polymer-based encapsulation *Nat. Energy* **4** 585–93
- [162] Conings B, Babayigit A and Boyen H-G 2019 Fire safety of lead halide perovskite photovoltaics *ACS Energy Lett.* **4** 873–8
- [163] Chen S, Deng Y, Gu H, Xu S, Wang S, Yu Z, Blum V and Huang J 2020 Trapping lead in perovskite solar modules with abundant and low-cost cation-exchange resins *Nat. Energy* **5** 1003–11
- [164] Wu S, Li Z, Li M-Q, Diao Y, Lin F, Liu T, Zhang J, Tieu P, Gao W and Qi F 2020 2D metal–organic framework for stable perovskite solar cells with minimized lead leakage *Nat. Nanotechnol.* **15** 934–40
- [165] Li X, Zhang F, He H, Berry J J, Zhu K and Xu T 2020 On-device lead sequestration for perovskite solar cells *Nature* **578** 555–8
- [166] Chen B, Fei C, Chen S, Gu H, Xiao X and Huang J 2021 Recycling lead and transparent conductors from perovskite solar modules *Nat. Commun.* **12** 1–10
- [167] Wang Q R, Lin Z H, Su J, Xu Y M, Guo X, Li Y C, Zhang M, Zhang J C, Chang J J and Hao Y 2022 Dithiol surface treatment towards improved charge transfer dynamic and reduced lead leakage in lead halide perovskite solar cells *Ecomat* **4** e12185
- [168] Liang Y M *et al* 2021 Lead leakage preventable fullerene-porphyrin dyad for efficient and stable perovskite solar cells *Adv. Funct. Mater.* **32** 2110139
- [169] Meng X *et al* 2021 A biomimetic self-shield interface for flexible perovskite solar cells with negligible lead leakage *Adv. Funct. Mater.* **31** 2106460
- [170] Zhang H, Li K, Sun M, Wang F L, Wang H and Jen A K Y 2021 Design of superhydrophobic surfaces for stable perovskite solar cells with reducing lead Leakage *Adv. Energy Mater.* **11** 2102281
- [171] Chen S, Deng Y, Xiao X, Xu S, Rudd P N and Huang J 2021 Preventing lead leakage with built-in resin layers for sustainable perovskite solar cells *Nat. Sustain.* **4** 636–43
- [172] Xu D, Mai R, Jiang Y, Chen C, Wang R, Xu Z, Kempa K, Zhou G, Liu J and Gao J 2022 An internal encapsulating layer for efficient, stable, repairable and low-lead-leakage perovskite solar cells *Energy Environ. Sci.* **15** 3891–900
- [173] Wu P and Zhang F 2022 Recent advances in lead chemisorption for perovskite solar cells *Trans. Tianjin Univ.* **28** 341–57
- [174] Ren M, Qian X, Chen Y, Wang T and Zhao Y 2022 Potential lead toxicity and leakage issues on lead halide perovskite photovoltaics *J. Hazard. Mater.* **426** 127848
- [175] Li X, Zhang F, Wang J X, Tong J H, Xu T and Zhu K 2021 On-device lead-absorbing tapes for sustainable perovskite solar cells *Nat. Sustain.* **4** 1038–41
- [176] Tian X, Stranks S D and You F 2021 Life cycle assessment of recycling strategies for perovskite photovoltaic modules *Nat. Sustain.* **4** 821–9
- [177] Kim B J, Kim D H, Kwon S L, Park S Y, Li Z, Zhu K and Jung H S 2016 Selective dissolution of halide perovskites as a step towards recycling solar cells *Nat. Commun.* **7** 1–9
- [178] Park S Y, Park J-S, Kim B J, Lee H, Walsh A, Zhu K, Kim D H and Jung H S 2020 Sustainable lead management in halide perovskite solar cells *Nat. Sustain.* **3** 1044–51
- [179] Ma S, Yuan G, Zhang Y, Yang N, Li Y and Chen Q 2022 Development of encapsulation strategies towards the commercialization of perovskite solar cells *Energy Environ. Sci.* **15** 13–55
- [180] Liu Z, Sun B, Shi T, Tang Z and Liao G 2016 Enhanced photovoltaic performance and stability of carbon counter electrode based perovskite solar cells encapsulated by PDMS *J. Mater. Chem. A* **4** 10700–9
- [181] Yoon J, Kim U, Choi J S, Choi M and Kang S M 2021 Bioinspired liquid-repelling sealing films for flexible perovskite solar cells *Mater. Today Energy* **20** 100622
- [182] Lv Y, Zhang H, Liu R, Sun Y and Huang W 2020 Composite encapsulation enabled superior comprehensive stability of perovskite solar cells *ACS Appl. Mater. Interfaces* **12** 27277–85
- [183] Idigoras J, Aparicio F J, Contreras-Bernal L, Ramos-Terron S, Alcaire M, Sanchez-Valencia J R, Borrás A, Barranco A and Anta J A 2018 Enhancing moisture and water resistance in perovskite solar cells by encapsulation with ultrathin plasma polymers *ACS Appl. Mater. Interfaces* **10** 11587–94
- [184] Fu Z *et al* 2019 Encapsulation of printable mesoscopic perovskite solar cells enables high temperature and long-term outdoor stability *Adv. Funct. Mater.* **29** 1809129
- [185] Dong Q, Liu F, Wong M K, Tam H W, Djurisić A B, Ng A, Surya C, Chan W K and Ng A M 2016 Encapsulation of perovskite solar cells for high humidity conditions *ChemSusChem* **9** 2597–603
- [186] Ma S *et al* 2020 1000 h operational lifetime perovskite solar cells by ambient melting encapsulation *Adv. Energy Mater.* **10** 1902472
- [187] Wong-Stringer M *et al* 2018 High-performance multilayer encapsulation for perovskite photovoltaics *Adv. Energy Mater.* **8** 1801234
- [188] Azar M H, Mohammadi M, Rezaei N T, Ayneband S and Simchi A 2022 Effect of silica encapsulation on the stability and photoluminescence emission of FAPbI<sub>3</sub> nanocrystals for white-light-emitting perovskite diodes *J. Alloys Compd.* **907** 164465
- [189] Wang J, Jia G, Kong H, Li H, Zuo R, Yang Y and Zhang C 2022 Highly efficient luminescence and enhanced stability of nanocomposites by encapsulating perovskite quantum dots in defect-related luminescent silica nanospheres *Appl. Surf. Sci.* **591** 153258
- [190] Gonzalez-Rodriguez R, Hathaway E, Lin Y, Coffey J L and Cui J 2022 Encapsulated MAPbBr<sub>3</sub> in nickel oxide

- nanotubes and their electroluminescence *Nanoscale* **14** 6417–24
- [191] Shi L *et al* 2017 Accelerated lifetime testing of organic-inorganic perovskite solar cells encapsulated by polyisobutylene *ACS Appl. Mater. Interfaces* **9** 25073–81
- [192] Emery Q, Remec M, Paramasivam G, Janke S, Dagar J, Ulbrich C, Schlattmann R, Stannowski B, Unger E and Khenkin M 2022 Encapsulation and outdoor testing of perovskite solar cells: comparing industrially relevant process with a simplified lab procedure *ACS Appl. Mater. Interfaces* **14** 5159–67
- [193] Zhao X, Liu T, Burlingame Q C, Liu T, Holley R, Cheng G, Yao N, Gao F and Loo Y-L 2022 Accelerated aging of all-inorganic, interface-stabilized perovskite solar cells *Science* **377** 307–10
- [194] Liu Z *et al* 2020 A holistic approach to interface stabilization for efficient perovskite solar modules with over 2,000-hour operational stability *Nat. Energy* **5** 596–604
- [195] Gong J, Adnani M, Jones B T, Xin Y, Wang S, Patel S V, Lochner E, Mattoussi H, Hu Y Y and Gao H 2022 Nanoscale encapsulation of hybrid perovskites using hybrid atomic layer deposition *J. Phys. Chem. Lett.* **13** 4082–9
- [196] Martins J, Emami S, Madureira R, Mendes J, Ivanou D and Mendes A 2020 Novel laser-assisted glass frit encapsulation for long-lifetime perovskite solar cells *J. Mater. Chem. A* **8** 20037–46
- [197] Li Z, Wu X, Wu S, Gao D, Dong H, Huang F, Hu X, Jen A K Y and Zhu Z 2022 An effective and economical encapsulation method for trapping lead leakage in rigid and flexible perovskite photovoltaics *Nano Energy* **93** 106853
- [198] Xiao X *et al* 2021 Lead-adsorbing ionogel-based encapsulation for impact-resistant, stable, and lead-safe perovskite modules *Sci. Adv.* **7** eabi8249
- [199] Kim J *et al* 2021 Lead-sealed stretchable underwater perovskite-based optoelectronics via self-recovering polymeric nanomaterials *ACS Nano* **15** 20127–35
- [200] Hu X, Li F and Song Y 2019 Wearable power source: a newfangled feasibility for perovskite photovoltaics *ACS Energy Lett.* **4** 1065–72
- [201] Yang D, Yang R, Priya S and Liu S F 2019 Recent advances in flexible perovskite solar cells: fabrication and applications *Angew. Chem., Int. Ed. Engl.* **58** 4466–83
- [202] Gao Y, Huang K, Long C, Ding Y, Chang J, Zhang D, Etgar L, Liu M, Zhang J and Yang J 2022 Flexible perovskite solar cells: from materials and device architectures to applications *ACS Energy Lett.* **7** 1412–45
- [203] Huang K, Peng Y, Gao Y, Shi J, Li H, Mo X, Huang H, Gao Y, Ding L and Yang J 2019 High-performance flexible perovskite solar cells via precise control of electron transport layer *Adv. Energy Mater.* **9** 1901419
- [204] Zhang Y, He P, Luo M, Xu X, Dai G and Yang J 2020 Highly stretchable polymer/silver nanowires composite sensor for human health monitoring *Nano Res.* **13** 919–26
- [205] Kumar A and Zhou C 2010 The race to replace tin-doped indium oxide: which material will win? *ACS Nano* **4** 11–14
- [206] Mutiari A, Dimopoulos T, Bauch M, Mittal A, Weil M and Wibowo R A 2021 Design and implementation of an ultrathin dielectric/metal/dielectric transparent electrode for  $\text{Cu}_2\text{ZnSnS}_4$  thin-film photovoltaics *Sol. Energy Mater. Sol. Cells* **230** 111247
- [207] Lee H J, Kim B-H, Takaloo A V, Son K R, Dongale T D, Lim K M and Kim T G 2021 Haze-suppressed transparent electrodes using IZO/Ag/IZO nanomesh for highly flexible and efficient blue organic light-emitting diodes *Adv. Opt. Mater.* **9** 2002010
- [208] Kim J-G, Na S-I and Kim H-K 2018 Flexible and transparent IWO films prepared by plasma arc ion plating for flexible perovskite solar cells *AIP Adv.* **8** 105122
- [209] Zhang J *et al* 2018 Stretchable transparent electrode arrays for simultaneous electrical and optical interrogation of neural circuits in vivo *Nano Lett.* **18** 2903–11
- [210] Wang Y, Lv Z, Chen J, Wang Z, Zhou Y, Zhou L, Chen X and Han S T 2018 Photonic synapses based on inorganic perovskite quantum dots for neuromorphic computing *Adv. Mater.* **30** 1802883
- [211] Lee G *et al* 2019 Ultra-flexible perovskite solar cells with crumpling durability: toward a wearable power source *Energy Environ. Sci.* **12** 3182–91
- [212] Worfolk B J, Andrews Sean C, Park S, Reinspach J, Liu N, Toney Michael F, Mannsfeld Stefan C B and Bao Z 2015 Ultrahigh electrical conductivity in solution-sheared polymeric transparent films *Proc. Natl Acad. Sci.* **112** 14138–43
- [213] Chen Z *et al* 2021 Flexible and transparent metal nanowire microelectrode arrays and interconnects for electrophysiology, optogenetics, and optical mapping *Adv. Mater. Technol.* **6** 2100225
- [214] Zhang C, Cai J, Liang C, Khan A and Li W-D 2019 Scalable fabrication of metallic nanofiber network via templated electrode position for flexible electronics *Adv. Funct. Mater.* **29** 1903123
- [215] Li H, Li X, Wang W, Huang J, Li J, Huang S, Fan B, Fang J and Song W 2019 Ultraflexible and biodegradable perovskite solar cells utilizing ultrathin cellophane paper substrates and  $\text{TiO}_2/\text{Ag}/\text{TiO}_2$  transparent electrodes *Sol. Energy* **188** 158–63
- [216] Pisoni S, Fu F, Widmer R, Carron R, Moser T, Groening O, Tiwari A N and Buecheler S 2018 Impact of interlayer application on band bending for improved electron extraction for efficient flexible perovskite mini-modules *Nano Energy* **49** 300–7
- [217] Zhang Q *et al* 2022 Large-diameter carbon nanotube transparent conductor overcoming performance–yield tradeoff *Adv. Funct. Mater.* **32** 2103397
- [218] Ullah S, Yang X, Ta H Q, Hasan M, Bachmatiuk A, Tokarska K, Trzebicka B, Fu L and Rummeli M H 2021 Graphene transfer methods: a review *Nano Res.* **14** 3756–72
- [219] Hu X *et al* 2019 A mechanically robust conducting polymer network electrode for efficient flexible perovskite solar cells *Joule* **3** 2205–18
- [220] Liu Q, Qiu J, Yang C, Zang L, Zhang G and Sakai E 2021 High-performance PVA/PEDOT:PSS hydrogel electrode for all-gel-state flexible supercapacitors *Adv. Mater. Technol.* **6** 2000919
- [221] Fan X, Nie W, Tsai H, Wang N, Huang H, Cheng Y, Wen R, Ma L, Yan F and Xia Y 2019 PEDOT:PSS for flexible and stretchable electronics: modifications, strategies, and applications *Adv. Sci.* **6** 1900813
- [222] Han J, Yang J, Gao W and Bai H 2021 Ice-templated, large-area silver nanowire pattern for flexible transparent electrode *Adv. Funct. Mater.* **31** 2010155
- [223] Huang Z, Hu X, Liu C, Tan L and Chen Y 2017 Nucleation and crystallization control via polyurethane to enhance the bendability of perovskite solar cells with excellent device performance *Adv. Funct. Mater.* **27** 1703061
- [224] Meng X, Xing Z, Hu X, Huang Z, Hu T, Tan L, Li F and Chen Y 2020 Stretchable perovskite solar cells with recoverable performance *Angew. Chem., Int. Ed. Engl.* **59** 16602–8
- [225] Lan Y, Wang Y, Lai Y, Cai Z, Tao M, Wang Y, Li M, Dong X and Song Y 2022 Thermally driven self-healing efficient flexible perovskite solar cells *Nano Energy* **100** 107523



- [226] Duan X, Li X, Tan L, Huang Z, Yang J, Liu G, Lin Z and Chen Y 2020 Controlling crystal growth via an autonomously longitudinal scaffold for planar perovskite solar cells *Adv. Mater.* **32** e2000617
- [227] Gutwald M, Rolston N, Printz A D, Zhao O, Elmaraghi H, Ding Y, Zhang J and Dauskardt R H 2020 Perspectives on intrinsic toughening strategies and passivation of perovskite films with organic additives *Sol. Energy Mater. Sol. Cells* **209** 110433
- [228] Jiang N, Xing B, Wang Y, Zhang H, Yin D, Liu Y, Bi Y, Zhang L, Feng J and Sun H 2022 Mechanically and operationally stable flexible inverted perovskite solar cells with 20.32% efficiency by a simple oligomer cross-linking method *Sci. Bull.* **67** 794–802
- [229] Ge C, Yang Z, Liu X, Song Y, Wang A and Dong Q 2021 Stable and highly flexible perovskite solar cells with power conversion efficiency approaching 20% by elastic grain boundary encapsulation *CCS Chem.* **3** 2035–44
- [230] Liu Y, Chen T, Jin Z, Li M, Zhang D, Duan L, Zhao Z and Wang C 2022 Tough, stable and self-healing luminescent perovskite-polymer matrix applicable to all harsh aquatic environments *Nat. Commun.* **13** 1338
- [231] Xu Y, Lin Z, Wei W, Hao Y, Liu S, Ouyang J and Chang J 2022 Recent progress of electrode materials for flexible perovskite solar cells *Nanomicro Lett.* **14** 117
- [232] Hu Y *et al* 2021 Flexible perovskite solar cells with high power-per-weight: progress, application, and perspectives *ACS Energy Lett.* **6** 2917–43
- [233] Jia C *et al* 2019 Highly flexible, robust, stable and high efficiency perovskite solar cells enabled by van der Waals epitaxy on mica substrate *Nano Energy* **60** 476–84
- [234] Gong C *et al* 2021 A non-wetting and conductive polyethylene dioxothiophene hole transport layer for scalable and flexible perovskite solar cells *Sci. China Chem.* **64** 834–43
- [235] Meng X *et al* 2020 Bio-inspired vertebral design for scalable and flexible perovskite solar cells *Nat. Commun.* **11** 3016
- [236] Dai Z, Yadavalli S K, Chen M, Abbaspourtamijani A, Qi Y and Padture N P 2021 Interfacial toughening with self-assembled monolayers enhances perovskite solar cell reliability *Science* **372** 618–22
- [237] Ochoa-Martinez E and Milić J V 2021 Get tougher *Nat. Energy* **6** 858–9
- [238] Bu T, Li J, Zheng F, Chen W, Wen X, Ku Z, Peng Y, Zhong J, Cheng Y-B and Huang F 2018 Universal passivation strategy to slot-die printed  $\text{SnO}_2$  for hysteresis-free efficient flexible perovskite solar module *Nat. Commun.* **9** 4609
- [239] Kim Y Y, Yang T Y, Suhonen R, Kemppainen A, Hwang K, Jeon N J and Seo J 2020 Roll-to-roll gravure-printed flexible perovskite solar cells using eco-friendly antisolvent bathing with wide processing window *Nat. Commun.* **11** 5146
- [240] Paik M J, Yoo J W, Park J, Noh E, Kim H, Ji S-G, Kim Y Y and Seok S I 2022  $\text{SnO}_2$ - $\text{TiO}_2$  hybrid electron transport layer for efficient and flexible perovskite solar cells *ACS Energy Lett.* **7** 1864–70
- [241] Wang H *et al* 2021 An in situ bifacial passivation strategy for flexible perovskite solar module with mechanical robustness by roll-to-roll fabrication *J. Mater. Chem. A* **9** 5759–68
- [242] Taheri B, De Rossi F, Lucarelli G, Castriotta L A, Di Carlo A, Brown T M and Brunetti F 2021 Laser-scribing optimization for sprayed  $\text{SnO}_2$ -based perovskite solar modules on flexible plastic substrates *ACS Appl. Energy Mater.* **4** 4507–18
- [243] Lei T *et al* 2020 Flexible perovskite solar modules with functional layers fully vacuum deposited *Sol. RRL* **4** 2000292
- [244] Castriotta L A, Fuentes Pineda R, Babu V, Spinelli P, Taheri B, Matteocci F, Brunetti F, Wojciechowski K and Di Carlo A 2021 Light-stable methylammonium-free inverted flexible perovskite solar modules on pet exceeding 10.5% on a 15.7  $\text{cm}^2$  active area *ACS Appl. Mater. Interfaces* **13** 29576–84
- [245] Hwang K, Jung Y S, Heo Y J, Scholes F H, Watkins S E, Subbiah J, Jones D J, Kim D Y and Vak D 2015 Toward large scale roll-to-roll production of fully printed perovskite solar cells *Adv. Mater.* **27** 1241–7
- [246] Yang X *et al* 2022 Scalable flexible perovskite solar cells based on a crystalline and printable template with intelligent temperature sensitivity *Sol. RRL* **6** 2100991
- [247] Fan B, Xiong J, Zhang Y, Gong C, Li F, Meng X, Hu X, Yuan Z, Wang F and Chen Y 2022 A bionic interface to suppress the coffee-ring effect for reliable and flexible perovskite modules with a near-90% yield rate *Adv. Mater.* **34** e2201840
- [248] Di Giacomo F *et al* 2015 Flexible perovskite photovoltaic modules and solar cells based on atomic layer deposited compact layers and uv-irradiated  $\text{TiO}_2$  scaffolds on plastic substrates *Adv. Energy Mater.* **5** 1401808
- [249] Yeo J-S, Lee C-H, Jang D, Lee S, Jo S M, Joh H-I and Kim D-Y 2016 Reduced graphene oxide-assisted crystallization of perovskite via solution-process for efficient and stable planar solar cells with module-scales *Nano Energy* **30** 667–76
- [250] Dagar J, Castro-Hermosa S, Gasbarri M, Palma A L, Cina L, Matteocci F, Calabrò E, Di Carlo A and Brown T M 2018 Efficient fully laser-patterned flexible perovskite modules and solar cells based on low-temperature solution-processed  $\text{SnO}_2$ /mesoporous- $\text{TiO}_2$  electron transport layers *Nano Res.* **11** 2669–81
- [251] Hu X *et al* 2019 Nacre-inspired crystallization and elastic “brick-and-mortar” structure for a wearable perovskite solar module *Energy Environ. Sci.* **12** 979–87
- [252] Ru P *et al* 2020 High electron affinity enables fast hole extraction for efficient flexible inverted perovskite solar cells *Adv. Energy Mater.* **10** 1903487
- [253] Chung J *et al* 2020 Record-efficiency flexible perovskite solar cell and module enabled by a porous-planar structure as an electron transport layer *Energy Environ. Sci.* **13** 4854–61
- [254] Li L *et al* 2022 Flexible all-perovskite tandem solar cells approaching 25% efficiency with molecule-bridged hole-selective contact *Nat. Energy* **7** 708–17
- [255] Kothandaraman R K *et al* 2022 Laser patterned flexible 4T perovskite-Cu(In,Ga)Se<sub>2</sub> tandem mini-module with over 18% efficiency *Sol. RRL* **6** 2200392
- [256] Li S, Xu L D and Zhao S 2015 The internet of things: a survey *Inform. Syst. Front.* **17** 243–59
- [257] Gasparini N, Salteo A, McCulloch I and Baran D 2019 The role of the third component in ternary organic solar cells *Nat. Rev. Mater.* **4** 229–42
- [258] Song D, Li M, Li Y, Zhao X, Jiang B and Jiang Y 2014 Highly transparent and efficient counter electrode using  $\text{SiO}_2$ /PEDOT-PSS composite for bifacial dye-sensitized solar cells *ACS Appl. Mater. Interfaces* **6** 7126–32
- [259] Yang C, Qu J and Wu Z 2021 Mechanical reliability of flexible encapsulation of III–V compound thin film solar cells *Sol. Energy* **214** 542–50
- [260] Kao M H, Shen C H, Yu P C, Huang W H, Chueh Y L and Shieh J M 2017 Low-temperature growth of hydrogenated amorphous silicon carbide solar cell by inductively

- coupled plasma deposition toward high conversion efficiency in indoor lighting *Sci. Rep.* **7** 12706
- [261] Ryu H S, Park S Y, Lee T H, Kim J Y and Woo H Y 2020 Recent progress in indoor organic photovoltaics *Nanoscale* **12** 5792–804
- [262] Xing Z, Lin S, Meng X, Hu T, Li D, Fan B, Cui Y, Li F, Hu X and Chen Y 2021 A highly tolerant printing for scalable and flexible perovskite solar cells *Adv. Funct. Mater.* **31** 2107726
- [263] Dong Q *et al* 2021 Flexible perovskite solar cells with simultaneously improved efficiency, operational stability, and mechanical reliability *Joule* **5** 1587–601
- [264] Deng Y, Zheng X, Bai Y, Wang Q, Zhao J and Huang J 2018 Surfactant-controlled ink drying enables high-speed deposition of perovskite films for efficient photovoltaic modules *Nat. Energy* **3** 560–6
- [265] Zuo C, Vak D, Angmo D, Ding L and Gao M 2018 One-step roll-to-roll air processed high efficiency perovskite solar cells *Nano Energy* **46** 185–92
- [266] Kim Y Y, Yang T Y, Suhonen R, Valimäki M, Maaninen T, Kemppainen A, Jeon N J and Seo J 2019 Gravure-printed flexible perovskite solar cells: toward roll-to-roll manufacturing *Adv. Sci.* **6** 1802094
- [267] Song Z, Chen C, Li C, Awni R A, Zhao D and Yan Y 2019 Wide-bandgap, low-bandgap, and tandem perovskite solar cells *Semicond. Sci. Technol.* **34** 093001
- [268] Kojima A, Teshima K, Shirai Y and Miyasaka T 2009 Organometal halide perovskites as visible-light sensitizers for photovoltaic cells *J. Am. Chem. Soc.* **131** 6050–1
- [269] Green M A 2016 Commercial progress and challenges for photovoltaics *Nat. Energy* **1** 15015
- [270] Venkateswararao A, Ho J K W, So S K, Liu S-W and Wong K-T 2020 Device characteristics and material developments of indoor photovoltaic devices *Mater. Sci. Eng. R* **139** 100517
- [271] Cui Y, Hong L, Zhang T, Meng H, Yan H, Gao F and Hou J 2021 Accurate photovoltaic measurement of organic cells for indoor applications *Joule* **5** 1016–23
- [272] Chen C-Y, Chang J-H, Chiang K-M, Lin H-L, Hsiao S-Y and Lin H-W 2015 Perovskite photovoltaics for dim-light applications *Adv. Funct. Mater.* **25** 7064–70
- [273] Li M *et al* 2018 Interface modification by ionic liquid: a promising candidate for indoor light harvesting and stability improvement of planar perovskite solar cells *Adv. Energy Mater.* **8** 1801509
- [274] He X, Chen J, Ren X, Zhang L, Liu Y, Feng J, Fang J, Zhao K and Liu S F 2021 40.1% Record low-light solar-cell efficiency by holistic trap-passivation using micrometer-thick perovskite film *Adv. Mater.* **33** e2100770
- [275] Wang K-L, Li X-M, Lou Y-H, Li M and Wang Z-K 2021 CsPbBr<sub>2</sub> perovskites with low energy loss for high-performance indoor and outdoor photovoltaics *Sci. Bull.* **66** 347–53
- [276] Wang K-L *et al* 2021 Smelting recrystallization of CsPbBr<sub>2</sub> perovskites for indoor and outdoor photovoltaics *eScience* **1** 53–59
- [277] Chen C H *et al* 2022 Full-dimensional grain boundary stress release for flexible perovskite indoor photovoltaics *Adv. Mater.* **34** e2200320
- [278] Yang W-F, Cao J-J, Dong C, Li M, Tian Q-S, Wang Z-K and Liao L-S 2021 Suppressed oxidation of tin perovskite by Catechin for eco-friendly indoor photovoltaics *Appl. Phys. Lett.* **118** 023501
- [279] Bi E *et al* 2019 Efficient perovskite solar cell modules with high stability enabled by iodide diffusion barriers *Joule* **3** 2748–60